CHALMERS
UNIVERSITY OF TECHNOLOGY

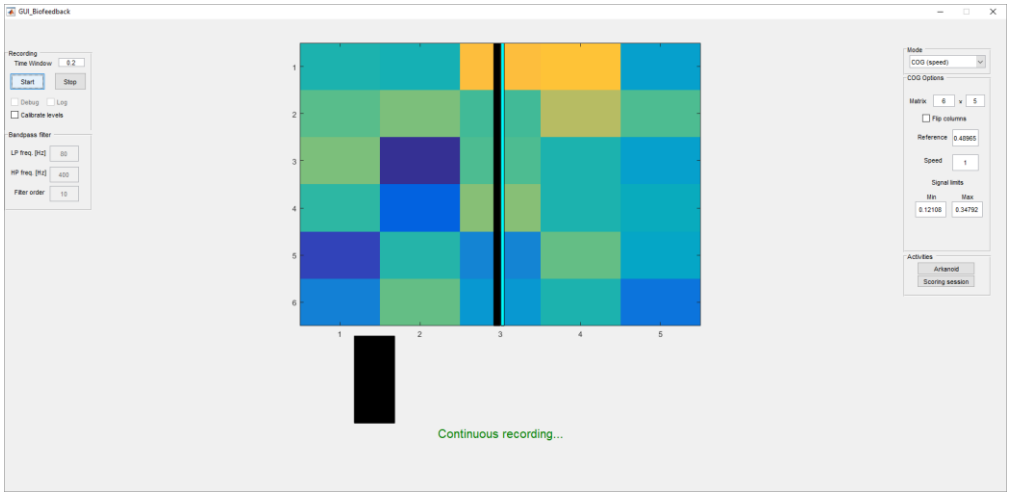

Differential activation using EMG biofeedback training

Master's thesis in Biomedical Engineering

Simon Nilsson

Department of Electrical Engineering

CHALMERS UNIVERSITY OF TECHNOLOGY

Gothenburg, Sweden 2017

MASTER'S THESIS IN BIOMEDICAL ENGINEERING

Differential activation using EMG biofeedback training

Simon Nilsson

Department of Electrical Engineering
CHALMERS UNIVERSITY OF TECHNOLOGY
Gothenburg, Sweden 2017

Differential activation using EMG biofeedback training

Simon Nilsson

Master's thesis SSYX04/2017

Department of Electrical Engineering

Chalmers University of Technology

SE-412 96 Göteborg

Sweden

Telephone: +46 (0)31 – 772 1000

Abstract

Myoelectric prostheses use muscular electrical signals as control input for the prosthesis. Certain of these muscles consist of two or more compartments, individually innervated by separate nerve branches. This thesis aims to investigate the mechanics behind the relative contribution of the compartments of such a muscle during movements, and whether it is possible to learn to voluntarily and independently activate them, to aid in the development of future prosthetic control strategies.

To achieve this, a study was performed on eight able-bodied subjects, using high density surface EMG to investigate the activation patterns of the biceps brachii. The activation patterns within the muscle was studied while the subjects performed eight movements of the lower arm. Voluntary differential activation of the compartments was studied by letting the subjects perform a training session within a purposely made biofeedback GUI, controlled by the amount of differential activation. The activation patterns were studied using the two-dimensional Centre-Of-Gravity (COG) of the spatial distribution of the muscular activation, while the level of differential activation was measured as the lateral COG of the spatial distribution of the muscular activation.

The results showed clustering in the task-specific COG for all subjects, indicating consistent patterns in activation patterns within the muscle during movements. These patterns appeared to be individual for each subject. In the differential activation training, most subjects were shown to have achieved improved control of the biofeedback GUI during the training session, possibly indicating that intentional and voluntary differential activation is possible to train.

Limitations in the surface EMG technology makes it difficult to establish for certain that the measured differential activation stems from separate activation of the compartments of the muscle. More sophisticated data processing algorithms or use of intramuscular EMG would be necessary to control for effects such as muscular cross-talk and displacement of the muscular bulk under the skin.

Acknowledgements

This project was far from a one-man show. I offer my sincerest gratitude to everybody who has helped and supported me along the way. Without your help I would not have made it to where I am.

Thank you, Eva and Max, who provided me with invaluable guidance throughout all the twists and turns of the project. You were the greatest supervisors one could wish for and made this thesis the incredible learning experience that it was.

Thank you, Enzo, Ale, Adam, Jake, Sonam and everybody else at BNL and Integrum, for enduring my endless questions and easing me into the world of electromyography. Without your expertise and company during long studying hours this project would not have been possible.

Thank you, test subjects, who endured my long and sometimes strenuous experiments with nothing more than my gratitude in return. You were incredibly patient and provided me with many insightful ideas on top of the data this thesis was founded on.

Thank you, Moa, for always being there for me. I would not have made it without your continuous support, love and valuable feedback. You mean the world to me.

Thank you, mum and dad, for always believing in me and supporting me. You are really what made me the engineer I am today.

Thank you, all my family and friends, who were my link to the outside world during the project. You allowed me to take my mind of the project and provided relief when it was most needed.

List of abbreviations

BB	Biceps brachii
COG	Centre of gravity
EMG	Electromyography
GUI	Graphical user interface
ID	Index of difficulty
HD-sEMG	High density surface electromyography
MT	Movement time (Fitts's law test repetition completion time)
MU	Motor unit
MVC	Maximum voluntary contraction
RMS	Root mean square
SDD	Standard distance deviation
SI	Separability index
SNR	Signal-to-noise ratio
TP	Throughput (Fitts's law test index of performance)

Anatomical directions

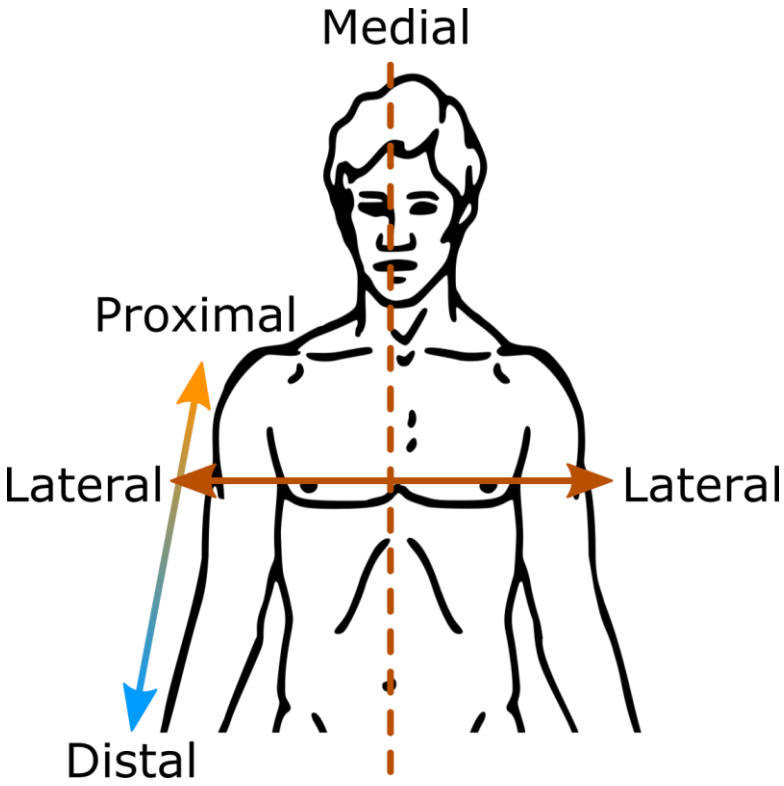

Figure 1: Illustration of anatomical directions used throughout the report. [1]

[1] *Adapted from work by NASA [Public domain], via Wikimedia Commons. Retrieved September 14, 2017 from https://commons.wikimedia.org/wiki/File:Line-drawing_of_a_human_man.svg*

Table of contents

1 Introduction

Losing an extremity, whether due to trauma or disease, is a life-changing event. The loss of a limb can be both a mental and physical handicap as the inability to perform tasks that previously were taken for granted is a mental burden that can lead to feelings of helplessness and loss of independence.

Humanity has long striven to find ways to regain the functionality of lost limbs. Replantation of the lost extremity can be an alternative, but this may not always be a possibility depending on the extent of the damage. Medical progress has made limb transplantations an increasingly realistic alternative, although problems such as immunosuppression and finding suitable replacement limbs make this treatment unavailable but for the select few [1]. Another approach is to replace the limb with an artificial version of it, a prosthesis. Up until recently, prostheses have been static attachments meant to improve aesthetics and replace simple functionality, such as wooden hands or a pirate's hook and peg leg. Functional prostheses aim instead to restore the functionality of the lost limb and are powered either mechanically or electrically. Advances in technology have allowed these electrical prostheses to become natural extensions of the patients' bodies with functionality approaching that of the original limb.

One kind of commonly used electrical prosthesis is the myoelectric prosthesis, which uses electrical signals from the remaining muscles of the limb as control input. A central challenge in the design of these prostheses is the fact that as the level of amputation increases, the number of limb functions to be replaced increases while the number of muscles to collect input signals from decreases. As most commercially available prostheses use a simple control strategy where each function is controlled by a single muscle, each lost muscular control site means one less function on the prosthesis.

It is obviously of major interest to maximise the number of independent muscular control sites to improve the functionality of the prosthesis. A possible venue for this would be learning how to control parts of a single muscle separately, so called differential activation. This could be possible since many of the human muscles consist of two or more compartments, each individually innervated by a motor neuron. If it was possible to learn voluntary differential activation, each compartment could potentially be used as a separate control site for the prosthesis.

The project was performed under the supervision of Eva Lendaro and Dr. Max Ortiz-Catalán at Chalmers University of Technology with the help and resources of Integrum AB.

1.1 Aim of the project

This thesis aims to perform a study to investigate the mechanics behind differential activation to aid in the development of future prosthetic control strategies. The investigations will focus both on subconscious separate activation of parts of a muscle when performing ordinary tasks as well as the possibility of training voluntary differential

activation. A literature study was also undertaken to get familiarised with the research area and the results of it is presented in this report.

1.2 Limitations

Measurements will only be performed on the Biceps Brachii (BB) muscle of the upper arm, although similar concepts should be applicable for other muscles with two or more heads. All electromyography measurements will be performed using surface electrodes.

2 Theory

This section presents some of the underlying concepts behind the used techniques and aims of this thesis. It also contains the results of the literature study, which includes both a brief history of myoelectrical prostheses as well as the current state-of-the-art both in myoelectric prosthesis control and EMG measurement techniques.

2.1 The anatomy behind differential activation

Skeletal muscles are used to stabilize the body and produce voluntary movements, and it is thus the functionality of these muscles that is to be replaced by a prosthesis. A skeletal muscle consists of thousands of muscle fibres, which are the long, cylindrical cells that shorten to make the muscle contract. The fibres are grouped into motor units (MUs) where each MU is controlled by a single motor neuron. Activation of the motor neuron makes all the fibres in the MU contract, making the MUs the smallest controllable subdivisions of muscle.

However, MUs are not the only subdivisions of the muscles. MUs can be grouped in muscular compartments, which may in turn make up muscular heads [2]. Examples of such muscles are the biceps brachii and the triceps brachii of the upper arm, consisting of two and three heads respectively, and the quadriceps femoris of the upper thigh, consisting of four heads. Such muscular compartments are individually supplied, or innervated, by separate branches of motor nerves, making them theoretically possible to activate separately from each other. The area of the muscle to which the motor neuron connects is referred to as the innervation zone. As can be seen in Figure 2, the two heads of the BB are called the short head and the long head, and are each innervated by a separate branch of the musculocutaneous nerve.

The objective of this thesis is to further investigate the mechanics behind differential activation of the compartments of the biceps brachii (BB), and whether it is possible to learn to incite voluntary differential activation. The BB was deemed a suitable candidate for a first investigation due to the simplicity of it having just two muscular heads and its involvement in several arm movements.

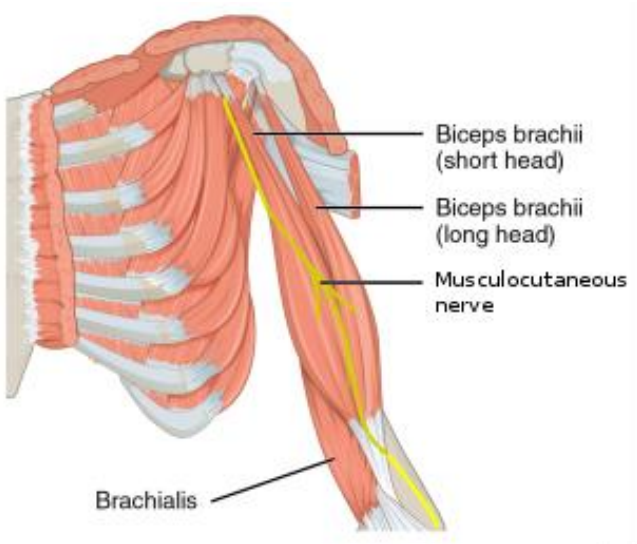

Figure 2: Separate branches of the musculocutaneous nerve innervate the two heads of the biceps brachii. [2]

2.2 The origin of myoelectric signals

A muscular contraction starts in the nervous system, through an electrical impulse known as the action potential. The action potential travels along a motor neuron until it reaches the neuromuscular junction, the meeting place between neuron and muscle. When the action potential reaches the neuromuscular junction, a chemical reaction takes place, signalling for the muscle to contract.

This chemical reaction gives rise to electrical signals travelling along the length of the muscle, muscular action potentials, much in the same way action potentials travel along the length of the motor neurons. The muscle fibres are made to contract by these muscular action potentials as they travel along the muscle fibres outwards from the innervation zone. These impulses give rise to measurable signals, so called myoelectric signals. The active muscle fibres can be viewed as a distributed bioelectric source located in a volume conductor consisting of other muscle fibres, blood vessels and connective tissue, making the signal propagate throughout the body. A recording of these signals is known as an electromyogram.

The electromyogram provides information about the contraction effort of the muscle it originates from. The frequency content ranges from about 25 Hz to several kHz, and when measured on the surface of the body the amplitude ranges from about 0.1 to 1 mV [3, p. 271]. It can be used both for diagnostic purposes and as control input for a prosthesis, or as in this project, to analyse the level of differential activation in a muscle.

---

[2] *Adapted from work by CFCF (Own work) [CC BY-SA 4.0 (http://creativecommons.org/licenses/by-sa/4.0)], via Wikimedia Commons. Retrieved September 14, 2017 from https://commons.wikimedia.org/wiki/File:1120_Muscles_that_Move_the_Forearm_Humerus_Flex_Sin.png*

2.3 Myoelectric prosthesis control

The basic principle behind myoelectric prostheses is to use the same signals that are collected in an EMG measurement to control a prosthesis. The very first myoelectric prosthesis was implanted in Russia in the early 1960s [4]. These early prostheses were limited by the electronics of the time, and the control strategy was limited to using the amplitude or the firing rate of the EMG to switch between two states. This approach required one channel per movement, so called 1-for-1 control, and the number of available degrees of freedom was limited by the number of independent muscular control sites. In the late '60s three-state amplitude modulated channels were developed, where each muscle source could control two different movements which were activated depending on the intensity of the EMG signal [5]. This approach allowed control of more functions, although prostheses using this technology were more complicated and a longer training period was required.

From 1975 and onwards much work has been performed to increase the performance and number of functions that can be controlled. Methods included to extract additional features of the EMG from each input channel as well as to increase the number of channels. Both these approaches yielded increased dimensionality of the EMG data which could be used as input to a classifier to determine which function to control, in an approach known as myoelectric pattern recognition.

Prosthetic control using a trained classifier for myoelectric pattern recognition has the benefit that the classifier can be trained to yield an intuitive control of the prosthesis, where the movements are performed as if they are natural movements of the missing limb. This is a major improvement compared to the unintuitive control of 1-for-1 prostheses where the muscular contractions required to control the prosthesis do not correspond to the performed movements, requiring long training periods for the subject. However, the classification can be computationally complex and introduce a delay in the control of the prosthesis. The classifier also needs to be trained to recognise the different movements to be performed and misclassifications due to variations in factors such as electrode repositioning and fatigue is a risk that has to be accounted for [6].

Even though the development of prostheses using pattern recognition have seen a lot of progress since their inception, most current clinically available prostheses still use conventional 1-for-1 control due to its simplicity and robustness [7]. Many different strategies have been developed to switch between functions to increase the number of functions beyond the number of control sites. Methods include switching between a sequential set of movements using a signal, such as simultaneous activation of two electrodes, or using movement triggers such as specific patterns of electrode activation to select certain movements. However, more control sites are always preferable to increase the number of simultaneously controllable functions as well as reduce the amount of switching needed. Introducing additional control sites through differential activation would thus be a large benefit in conventional prosthesis control.

2.4 High-density electromyography

To benefit from the electromyogram, it needs to be collected in a proper manner. The technique of measuring an electromyogram is called electromyography (EMG) and can be performed either by measuring the potential on the surface of the body using surface electrodes, or directly on the muscle using needle electrodes. Needle electrodes allow more precise measurements closer to the source; however, it is an invasive technique and needs to be performed by trained physicians. EMG using surface electrodes, so called surface EMG (sEMG), is a safe and non-invasive technique, although lower Signal-to-Noise Ratio (SNR) and increased distance from the source demand more careful signal processing. Cross-talk, where signals from adjacent muscles propagate to be picked up by nearby electrodes, is an issue that can make a source separation algorithm necessary for precise measurements.

Another consideration is whether to record in bipolar or monopolar configuration, as seen in Figure 3. In the bipolar configuration, the electrodes are paired, and each measurement channel is the difference in potential between an electrode pair. In the monopolar configuration, a single reference electrode is used, preferably placed in an area without EMG activity. Each measurement channel is then the potential difference between a measurement electrode and the reference electrode. Bipolar measurements have a higher SNR as the noise components common to both electrodes are eliminated, but the collected signal is affected by the distance between the two electrodes, making measurements more difficult to compare between experiments and subjects.

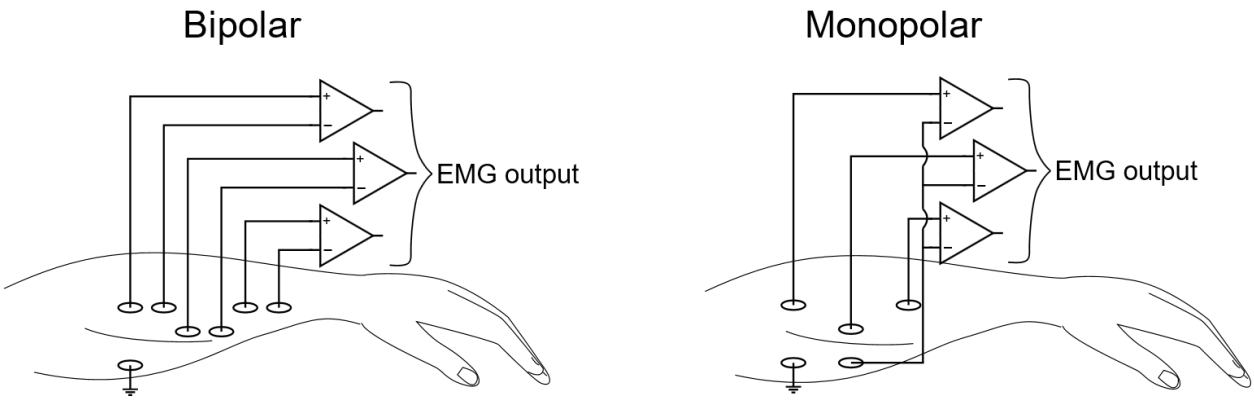

Figure 3: The difference between electromyography using bipolar and monopolar configuration

For the purposes of this project the EMG was performed using high-density surface electromyography (HD-sEMG), which uses many surface electrodes in monopolar configuration placed in a dense array as seen in Figure 4. Although HD-sEMG is a relatively novel technique, it offers an increased possibility to collect information about the spatial distribution of the EMG, as opposed to the mostly temporal information collected by conventional techniques. This added spatial information makes it ideal for measuring differential activation without having to use intramuscular electrodes.

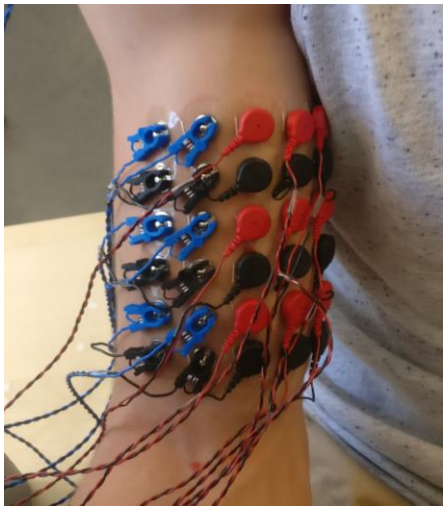

Figure 4: Example of a high-density surface electromyography electrode matrix and measurement leads attached to the biceps brachii of a subject.

2.5 Analysis of HD-sEMG measurements

The additional information gained from HD-sEMG measurements comes at the cost of complexity, as the significant amount of collected data requires proper data analysis techniques to provide useful results. However, a simple method to visualise the data is by rendering HD-sEMG maps from the measurements. This is commonly performed by visualising the electrode matrix as an image, where each pixel corresponds to the RMS activity of a channel during a specified time window as seen in Figure 7 [8]–[13].

Visualisation in the form of HD-sEMG maps allows distinguishing separate activation areas, such as different muscles or compartments within a single muscle, as the activation areas yield clusters of high-intensity pixels in the HD-sEMG maps [11]. This method yields images that provide an easily understandable overview of the muscular activation patterns and further data analysis can be performed by comparing pixel values of the generated maps.

2.6 Earlier studies of differential activation in the biceps brachii

The study of differential activation within the BB is a relatively new subject. In 1983 Haar Romeny et al. showed the functional difference of MUs in the long head of the BB [14]. They showed how individual MUs had different firing levels during supination of the forearm and flexion of the elbow, and how these various kinds of MUs were grouped medially or laterally depending on their function. The anatomical basis for these findings were confirmed by Segal in 1992, who by examining BB specimens discovered the existence of between two and four parallel individually innervated muscular compartments in each head of the BB [2]. In 1993 Brown et al. went on to investigate the amount of differential activation of the BB during rapid supination movements, and found that joint position had a significant effect on the relative activation of the two heads of the muscle [15].

Since then much work has been performed to increase the understanding of the mechanisms behind differential activation of the BB. It has been shown that the two heads contribute to different amounts to supination and flexion, however, the relative differences

vary largely between subjects [16]. The amount of differential activation have also been shown to vary between concentric, isometric and eccentric contraction [17]. Neither resistance training nor aging seems to have an effect on the differential activation [18], [19], however, it has been shown that muscular fatigue primarily affects the EMG of the long head of the BB [20]. Earlier studies have shown that the effects of muscular fatigue on the EMG of the BB can persist for more than 25 hours [21].

All in all, there seems to be a complicated functional relationship between the two heads of the BB. However, the current consensus seems to be that arm posture has a major impact on the amount of differential activation, perhaps due to changes in biomechanical factors making activation of one head preferential over the other [15]. This was confirmed in a thesis by Nejat Nahal from which much inspiration was drawn for this thesis, where once again it was shown that changes in arm posture has a large impact on the relative activation of the two heads [22]. In fact, in a follow-up to Nejats thesis Aghajamaliaval showed that the different hand postures used in Nejats thesis seemed to have a negligible effect on the differential activation and the major decider was the arm posture [23].

2.7 Biofeedback training

A possible venue to allow training of differential activation is the usage of biofeedback training. Biofeedback is the technique of providing feedback of physiological parameters to a subject with the aim to increase the subject's control over bodily functions. Biofeedback training has been used to treat conditions such as anxiety, headaches and muscular tension [24] and has also shown promising results regarding training of differential muscle activation [9]. By visualising the electrical signals from the muscle to the subject as exemplified in Figure 5, so called EMG biofeedback, it is possible to gain immediate feedback about the amount of differential activation. It is this immediate feedback of changes in parameters normally outside of human sensation that has proven so valuable in biofeedback training.

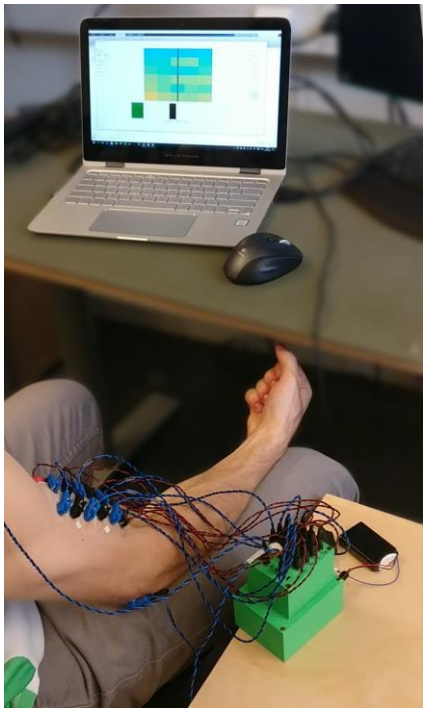

Figure 5: A subject controlling a biofeedback GUI under live feedback of the current activation of the muscle.

Biofeedback training using EMG has been shown to allow training of preferential activation of one muscle over another [25]. However, the usage of biofeedback training for enabling differential activation in a single muscle is relatively unexplored. Nonetheless, Holtermann et al. saw success in training differential activation of the four compartments of the trapezius muscle for several subjects during a one hour biofeedback training session [9]. This result shows the viability of using EMG biofeedback training to enable differential activation of the BB during relatively short training sessions.

2.8 Fitts's law test

Fitts's law is an empirical model predicting the time to point to a target area as a function of the distance and width of the target [26]. The model proposes that the time to reach the target is linearly dependent on the Index of Difficulty (ID) of the target, computed as

$$ID = \log_2\left(\frac{2D}{W}\right)$$

where D is the distance to the target, W is the width of the target and ID is the index of difficulty in bits. The law has been shown to hold true for many different pointing tasks, both physical pointing tasks and virtual ones using computer interfaces.

As such, tests using Fitts's law have been used to characterise the performance of different pointing interfaces. Such tests consist of a series of several targets with specified distances and widths to reach, and have been performed in up to three degrees of freedom at once. The tests may include a timeout, the maximum time to reach the target, and a dwell time, the time the cursor needs to stay in the target to consider the target reached. Such tests compute the Throughput (TP) of an interface as a function of their index of difficulty as

$$TP = \frac{1}{N}\sum_{i=1}^{N}\frac{ID_i}{MT_i}$$

often combined with several other performance metrics. Here N is the number of tasks in the test, MT_i is the movement time i.e. the time in seconds to reach target i while ID_i is its index of difficulty. These metrics may include completion rate (percentage of targets successfully reached), overshoot (average number of times the target was entered but then lost), efficiency (ratio of the distance of the optimal path to the target and the distance of the path taken) and stopping distance (distance travelled within the target). In this project, a Fitts's law test was used to help determine the subjects' level of control using differential activation and their improvement during training.

2.9 BioPatRec

All the GUIs developed in this thesis were developed within the framework of BioPatRec, a modular research platform developed in Matlab by Max Ortiz-Catalán, Rickard Brånemark, Bo Håkansson and many other contributors during the years [27]. The framework gave access to many different filtering and signal processing algorithms used during the thesis, as well as an interface to collect data using many different acquisition systems. BioPatRec is freely available on GitHub [28], where it is also possible to find a data repository of myoelectric recording sessions for development and experimentation. All software developed in this project will be integrated with and freely available through BioPatRec.

3 Method

This chapter describes the literature study and experiments to investigate the mechanics behind involuntary and voluntary differential activation of the BB. It also presents what hardware was used and the software that was developed for use in the study.

3.1 Literature study

The literature study was performed by finding papers and theses on the search engines Google Scholar and the Chalmers' library search engine using the keywords "myoelectric pattern recognition", "HD-EMG", "high-density EMG", "differential activation", "biofeedback training", "review" "transhumeral", "upper arm", "biceps brachii", "EMG", "signal processing" and "targeted muscle reinnervation". The titles of the found papers were scanned to filter out irrelevant results. The abstracts of the remaining papers were then read to determine which papers were highly relevant to the subject. If relevant papers were found as citations in other papers these were also studied. In total, 62 papers and theses were selected and studied closer.

3.2 Hardware

The EMG was measured using a RHA2132 32-channel monopolar amplifier with an amplification of 200 V/V and separated grounding and reference connections, seen in Figure 6. The data was sampled using a custom-built ADC circuit provided by Integrum AB at a rate of 1000 samples/s per channel over USB by a PC using Matlab version R2015b [27]. The measurement, grounding and reference electrodes were single-use adhesive pre-gelled Ag/AgCl electrodes.

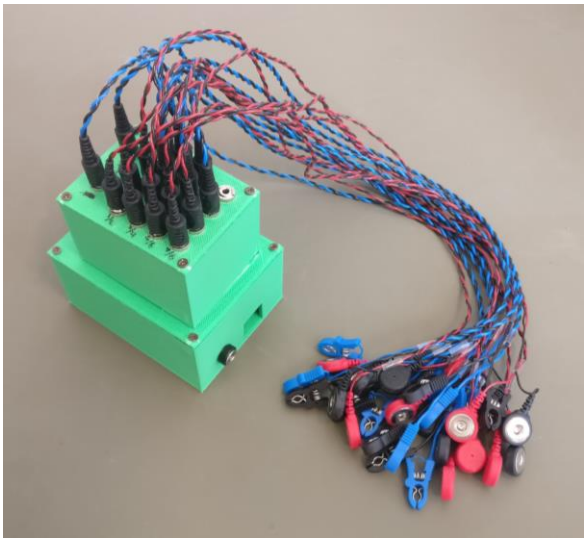

Figure 6: The 32-channel measurement amplifier in its casing.

The data was collected and transferred to the PC using a Texas Instruments TM4C123G microcontroller. Two different data acquisition modes were used during the experiments. During the pattern measurements, a continuous recording mode was used to ensure that

there were no gaps in the data received by the PC. During the biofeedback training a request-collect mode was used, where time windows of samples were recorded and transmitted only as requested by the PC. This acquisition mode was more robust and suitable for the long biofeedback training sessions where the timing of the time windows wasn't essential.

3.3 Data treatment algorithms

This section describes data treatment concepts frequently used in this project.

3.3.1 Generation of high density EMG maps

All the data processing was performed on HD-sEMG maps, rather than the raw collected EMG data. Figure 7 shows the process of forming such a map from a time window of samples. The first step is calculating the RMS of each channel during the time window. These RMS values were then assigned to a matrix of the same size as the electrode matrix, meaning that each element of the matrix represented the mean activation of the corresponding electrode during the time window. These matrices, or maps, were used both for the data analysis and to visualise the muscular activation patterns. The notation $M(i, j)$ is used throughout the thesis to denote the pixel value at row i and column j of the HD-sEMG map M.

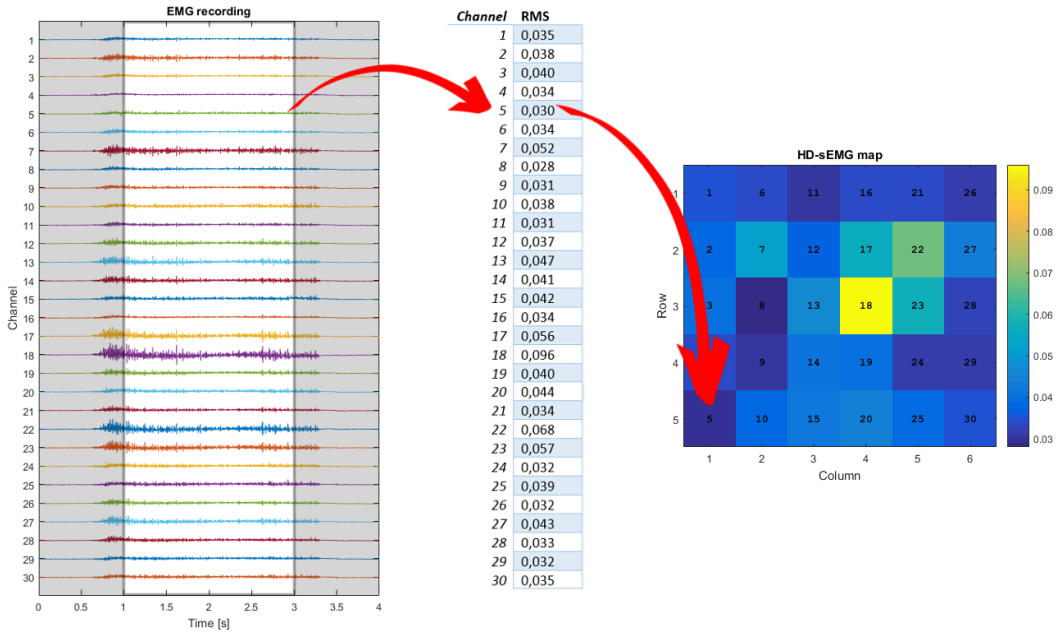

Figure 7: Generation of a high-density surface electromyography (HD-sEMG) map from a time window of samples. The beginning and the end of the contraction is discarded, the RMS of the remaining part is calculated and visualised in a grid corresponding to the electrode matrix.

3.3.2 Calculation of centre of gravity

To quantify the level of differential activation of an HD-sEMG map the lateral Centre-Of-Gravity (COG) of the HD-sEMG maps were computed. The longitudinal COG was also calculated and used for visualising the COG differences between tasks. The lateral and longitudinal COGs were calculated as

$$COG_{lat} = \frac{\sum_{(i,j)} jM(i,j)}{\sum_{(i,j)} M(i,j)}, COG_{long} = \frac{\sum_{(i,j)} iM(i,j)}{\sum_{(i,j)} M(i,j)}.$$

Here *M(i,j)* is the pixel value at position row *i* and column *j* of the HD-sEMG map and the COGs were computed in pixels.

3.4 Software

The two GUIs described in this section were developed as part of the project to visualise and treat HD-sEMG measurements and to be able to perform biofeedback training.

3.4.1 The high-density surface EMG GUI

A specialised GUI, based on a foundation developed by Max Ortiz-Catalán, was developed to visualise the substantial amounts of data collected in an HD-sEMG measurement session. Simply called the "HD-EMG GUI" as seen in Figure 8, the GUI allows calculation and visualisation of HD-sEMG maps as described in Section 3.3.1. By loading a previous recording session and defining filter, time window and spatial segmentation settings to use, the data can be pre-processed and played back in a movie format and the COG can be calculated and shown overlaid the map. Data can also be recorded directly in the GUI.

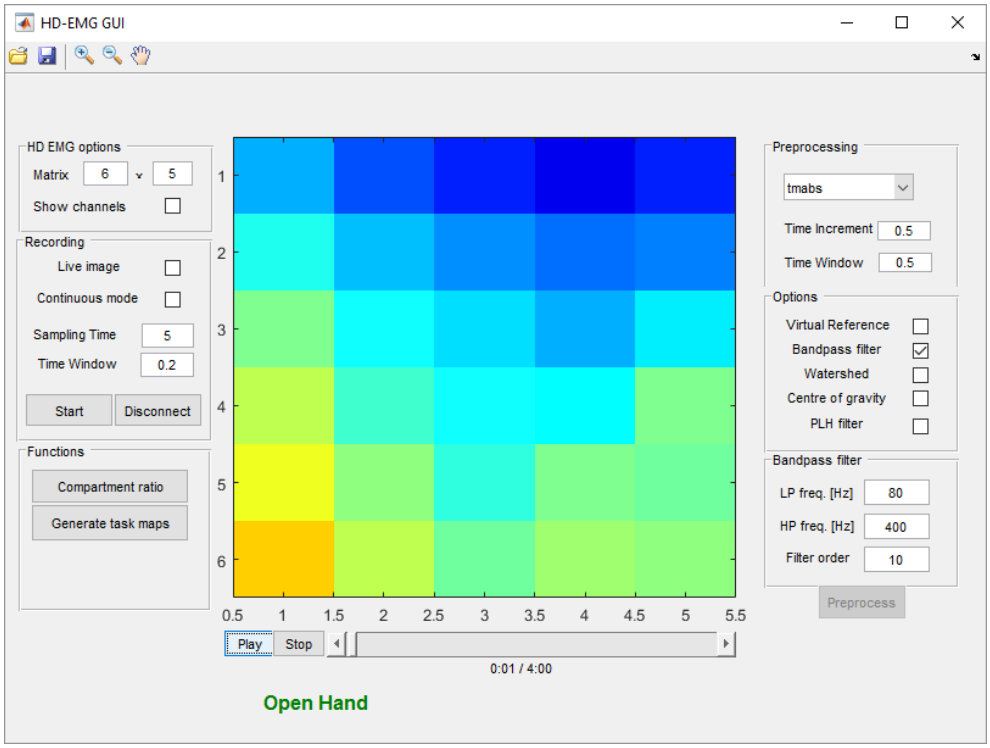

Figure 8: The HD-EMG GUI showing a high-density EMG map visualising the "tmabs" feature, corresponding to the RMS of each input channel during a time window.

The GUI was developed in the framework of BioPatRec to allow simple extraction of all the features of the EMG signals implemented in BioPatRec. The GUI was developed to handle the recording session format utilised in BioPatRec as well as recording using all the acquisition systems defined in BioPatRec.

3.4.2 The Biofeedback GUI

A purposely built GUI, developed in the BioPatRec framework, was developed to be able to perform biofeedback EMG training. As seen in Figure 9, the main parts of the GUI consisted of the moving bar, the reference bar, the COG bar and the HD-sEMG map. The HD-sEMG map showed the instantaneous HD-sEMG map calculated for the last collected time window, while the COG bar showed the lateral COG calculated for the map. The reference bar is stationary and can be set either manually or through calibration, representing neutral differential activation.

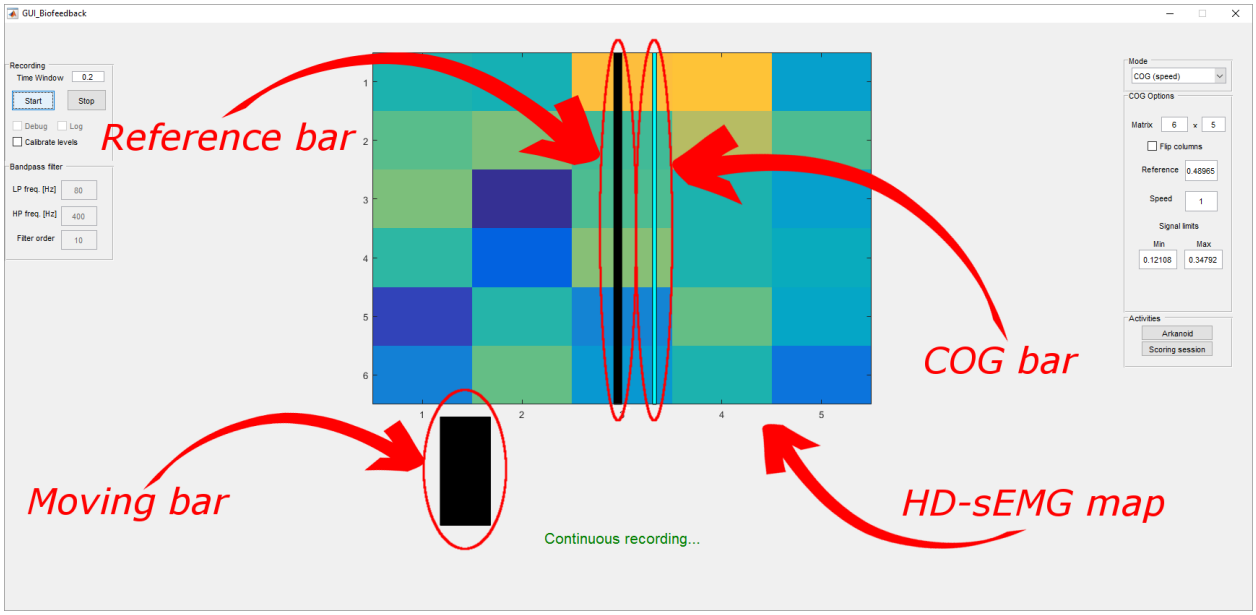

Figure 9: The Biofeedback GUI and its four main components, the reference bar, the COG bar, the moving bar and the HD-sEMG map.

The training works by moving the moving bar back and forth by inciting differential activation of the BB, measured as the distance between the COG bar and the reference bar. The goal is to obtain an intuitive control of the moving bar with speed proportional to the amount of current differential activation and encouraging improvement of the amount of differential activation by performing activities within the GUI.

The speed of the bar is updated at a selectable interval, referred to as the time window. Every time window, the EMG from all channels is recorded and filtered through a Butterworth bandpass filter with parameters selectable in the GUI. The RMS of each channel of the filtered signal is used to form the HD-sEMG map $M_k(i,j)$ for time window k which is then displayed in the GUI. This HD-sEMG map is then used to compute the lateral COG as described in Section 3.3.2, which is then shown by the position of the COG bar. A strength multiplier S_k is also computed for the HD-EMG map as

$$S_k = \frac{\frac{1}{N}\sum_{(i,j)} |M_k(i,j)| - S_{min}}{S_{max} - S_{min}}.$$

Here N is the number of channels while S_{min} and S_{max} are minimum and maximum signal levels, either set manually or through calibration. This strength multiplier represents the

relative strength of the contraction and is used to regulate the speed of the moving bar to make it move faster during stronger contractions, aiding in achieving intuitive control.

The distance between the computed lateral COG, COG_k, and the reference lateral COG, COG_R, and the strength multiplier S_k is then used to determine the speed v_k of the moving bar during time window $k + 1$ as

$$v_{k+1} = M \cdot {S_k}^2 (COG_k - COG_R).$$

M is a speed multiplier settable in the GUI for fine-tuning the speed of the bar. The effect is that the speed of the bar is controlled by both the displacement of the COG and the strength of the contraction, meaning that the subject must actively perform contractions with different amounts of differential activation to control the GUI. The algorithms for calculating the strength multiplier and the speed of the moving bar were developed empirically to give an intuitive feel of moving the bar. The squaring of the strength multiplier in the speed calculation is meant to give a sharp reduction of speed for low contraction levels, allowing fine control of the bar.

As mentioned, a built-in calibration function of the GUI can be used to find the reference COG and set appropriate signal levels. The calibration works by first calculating the average COG for five seconds to set the reference COG, COG_R, during which the subject is asked to perform a moderate flexion of the elbow with the forearm neutrally pronated. This is followed by measuring the average signal strength during two times three seconds to set first S_{min} and then S_{max}, during which the subject is asked to relax and then to perform moderate elbow flexion respectively. All calibrated parameters can be manually adjusted in the GUI afterwards.

Apart from the features mentioned above, the GUI also includes tests and games to measure the differential activation proficiency of the subject and to keep the subject engaged. These activities consist of a goal game, a Fitts's law test and a Breakout game where the subjects could control the paddle in the same way as the moving bar. The GUI also features logging to save the HD-sEMG maps and the logs from the activities for later analysis. The goal game and the Fitts's law test are described in more detail in the following sections.

3.4.2.1 Biofeedback goal game

The first of the activities in the biofeedback GUI is the goal game, designed to help evaluate the level of proficiency in differential activation. The goal game is structured as a series of levels of increasing difficulty. The goal of each level is to move the moving bar to a randomly generated goal area as seen in Figure 10 and keep it there for a dwell time of two seconds before the level timer runs out, as inspired by the TAC test [27]. The first level has a time limit of 12 seconds. As the session progresses, the time to complete each level decreases by 0.5 seconds to a minimum of three seconds at level 19 and onwards. When the subject fails to complete a level, the goal game concludes and the score is calculated as the number of successfully completed levels.

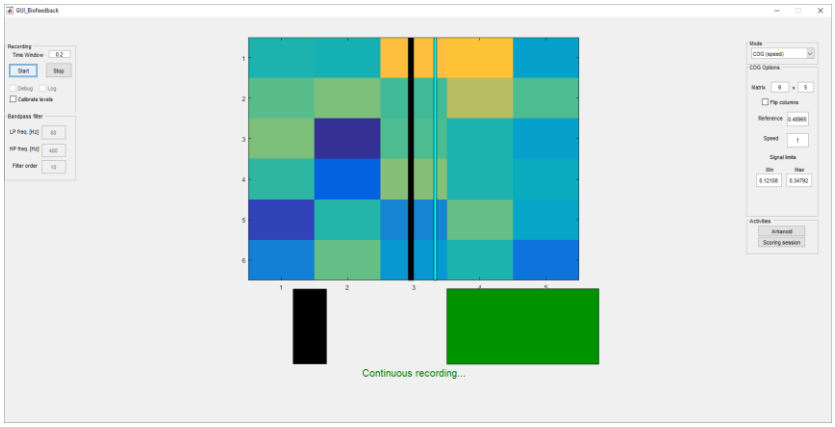

Figure 10: The goal game activity of the Biofeedback GUI. The goal of the game is to move the bar to the green goal area.

3.4.2.2 Biofeedback Fitts's law test

The other main activity of the biofeedback GUI is the Fitts's law test, to serve as a standardised method of testing the performance of the subject as described in Section 2.8. The concept of the test is the same as for the goal game, to move the moving bar to goal areas and keep it there for a specified dwell time. The differences are that the bar is centred before each repetition, the distance D and width W of each goal is specified beforehand and the test does not end if the repetition times out. All the metrics describes in Section 2.8 are measured and collected during the test, i.e. the completion rate, efficiency, stopping distance and overshoot.

To keep in accordance with Fitts's law test standards, the distances D and widths W of the targets are given in degrees, which in this instance are defined so that the range of motion of the moving bar is between -100 and 100 degrees. This can be seen in Figure 11, which also shows how D is defined as the distance between the starting point of the moving bar and the centre of the target while W is the difference between the width of the target and the width of the moving bar, i.e. the distance the bar can move while still remaining inside the target. The exact definition of the distance measure is not too important, as all metrics are computed using ratios of distances and widths. The distances in the default test in the GUI are 60, -30, 30, 60 degrees and the widths are 13 and 18 degrees. Two trials are performed, resulting in 16 repetitions for each test (four distances for each of two widths, repeated two times). The timeout is set to 15 seconds and the dwell time to one second.

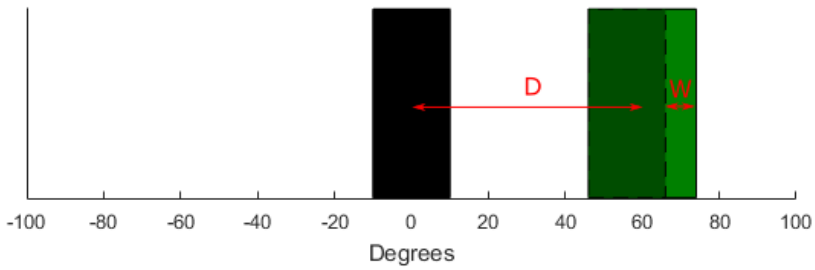

Figure 11: Definitions of distance D and width W of the Fitts's law test targets. D is the distance from the starting point to the centre of the target while W is the difference between the width of the target and the width of the moving bar.

3.5 Design of the differential activation experiments

This section describes the procedure and setup for the two different experiments performed in the study utilising the hardware and software described above.

3.5.1 Subject selection

Eight able-bodied subjects participated in the study. Only subjects without any previous muscular injuries in the BB of their dominant arm were selected. The age, gender, workout regime and dominant arm were collected for use in future statistical analyses. Every subject signed a form of informed consent after having the procedure explained to them.

3.5.2 Experimental setup

The experiment was performed in the Biomechatronics and Neurorehabilitation Laboratory at Chalmers University of Technology. The subjects were seated in a regular office chair without armrests during most of the experiment to allow for free movement of the arm. During parts of the experiment where the arm was fixated the subjects were instead sat in an office chair with armrests to which the arm was fixated using a bandage as seen in Figure 13. A 42-inch widescreen TV or a 24-inch computer monitor was used to present the GUIs to the subject, according to whichever display they found more comfortable using.

3.5.3 Preparations

After informing the subject about the procedure, the medial acromion and fossa cubit of the subject's dominant arm were located and the distance between these landmarks was measured and recorded for normalisation. A line was drawn between the landmarks and the centre mark for the electrode matrix was placed along this line at one third of the line's length from the fossa cubit. The arm circumference was measured around this mark and recorded. These landmarks and electrode placements were chosen in accordance with the result of the SENIAM project [29].

The BB of the dominant arm was covered with a 5x6 electrode matrix around the mark as indicated by Figure 12. The matrix had an inter-electrode distance of approximately 15 mm and slight deviations from the marked position were accepted to ensure optimal coverage of the BB, which was located by palpation. The two reference electrodes were placed on bony parts of the shoulder while the two ground electrodes were placed on the elbow to ensure placement over areas with low myoelectric activity and proper separation between ground and reference electrodes. The precise dimensions and placement of the electrode matrix were measured and recorded. To give the electrochemical interface between electrode and skin time to properly settle the subject had to wait 15 minutes between applying the electrodes and starting the measurements.

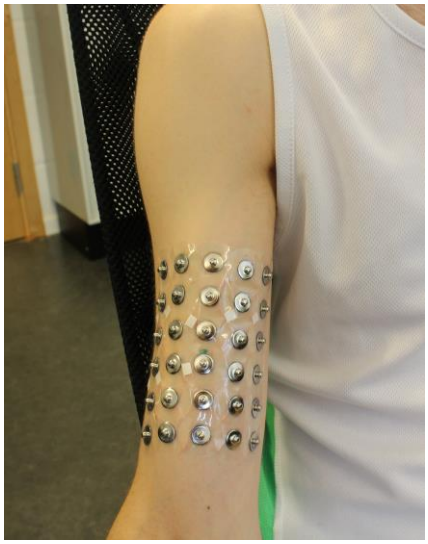

Figure 12: Placement of the electrode matrix on the biceps brachii.

Before starting the experiment, each subject performed an elbow flexion ramp recording using the built-in functionality of BioPatRec. This recording was used both to record the elbow flexion MVC for use in the data analysis and to verify good signal quality and muscle coverage. The ramp recording was performed with the forearm neutrally rotated with the elbow 90° flexed with the desk of the laboratory used to brace the forearm. Two five second contractions were performed with 20 seconds of rest in between.

3.5.4 Experimental procedure

The experiment consisted of three main parts to investigate the mechanics behind both involuntary and voluntary differential activation.

The first part was a set of pattern measurements during which the subjects performed eight tasks of the lower arm while the EMG was being recorded to investigate the level of differential activation during these tasks.

The second part was a biofeedback training session during which the subject could move their arm freely to determine the viability of the biofeedback training and the possibility of learning to incite voluntary differential activation.

The third part was another biofeedback training session where the subject had their arm fixated. The intention of this second training session was to minimize the effects of skin stretching and sliding of the muscles under the skin, shifting the active area with respect to the electrodes. The intent was to leave only the neural drive of the BB to control the GUI.

The following sections describe the parts in more detail.

3.5.4.1 Pattern measurements

The pattern measurements were performed using the “Recording Session” GUI of BioPatRec. The measurements consisted of the tasks shown in Table 1, eight tasks in total. No control of the contraction force was performed but the subject was asked to contract at roughly 70% of MVC. All tasks except the elbow extension and flexion were performed with the forearm resting in the lap of the subject to avoid any activation of the BB from keeping

the forearm elevated. Elbow extension and flexion were performed isometrically with the forearm neutrally pronated and the elbow approximately 90° flexed using the desk to brace the movement.

Table 1: Tasks performed during pattern measurements

Hand opening
Hand closing
Hand extension
Hand flexion
Forearm pronation
Forearm supination
Elbow extension
Elbow flexion

Using the recording session functionality of BioPatRec, each task was repeated five times with a contraction time of three seconds and three seconds of rest in between contractions with an added non-recorded dummy contraction to help prepare the subject. The recording session was performed three times in total to allow the subject to get used to the recording procedure and only the results from the last session were used. Faulty measurements were rerecorded to ensure all tasks were performed properly and as similarly as possible.

3.5.4.2 Biofeedback training without fixation of the arm

The biofeedback training was performed within the biofeedback GUI described in Section 3.4.2. The time window was set to 0.2 seconds. Each time window of samples was filtered using a 10th order Butterworth bandpass filter with cut-off frequencies 80Hz and 400Hz.

The built-in calibration function of the GUI was used to find the reference COG COG_R and set the appropriate signal levels S_{min} and S_{max} as described in Section 3.4.2. If needed, the calibration was repeated or the parameters were manually adjusted to achieve a comfortable control of the moving black bar.

After calibration of the GUI training session took place for approximately 40 minutes, alternating between free-form training and scoring sessions with a schedule as seen in Table 2. The training session ended after the third scoring session was finished.

Table 2: The schedule of the biofeedback training session.

Free-form training
Scoring session @ 5 minutes
Free-form training
Scoring session @ 20 minutes
Free-form training
Scoring session @ 35 minutes

The scoring sessions were performed throughout the training session to both measure its effects and serve as a method of practice, and each consisted of two goal games and one Fitts's law test as described in Section 3.4.2.1 and 3.4.2.2. When a scoring session was not taking place, the subject could move the moving bar back and forth at their leisure to try to improve the differential activation at their own pace. To keep the subject engaged they also had the possibility to launch the goal game and the Breakout game at will.

The subject was encouraged to experiment and vary parameters such as posture of the arm and contraction strength to increase the amount of differential activation and maximise their score. Otherwise no direction was given as how to perform the training.

Both the performed activities (scoring sessions and gameplay sessions) and the HD-sEMG maps were logged on the hard-drive of the PC. The three scheduled training sessions were filmed to allow visual inspection of the techniques employed by the subjects to perform the differential activation.

3.5.4.3 Biofeedback training session with fixated arm

The second biofeedback training session was similar to the first one but with the subject sat in a chair with armrests and the forearm fixated to the armrest of the chair as seen in Figure 13. The subject was instructed to keep their back towards the backrest of the chair. Apart from these differences the session was conducted in the same way as the regular training session described in Section 3.5.4.2. This session was intended to eliminate the effects of skin stretching and sliding of the muscles under the skin to ensure that the measured differential activation came purely from the neural drive of the BB.

Figure 13: A subject with their arm fixated during the training session with fixated arm. The forearm is wrapped tightly to the armrest of an sturdy office chair using a bandage.

3.6 Data analysis

The data analysis of the activation patterns (part one of the experiment) consisted of studying differences and similarities in the levels of differential activation between subjects by computing the lateral centres of gravity (COG) for the different tasks. The activation patterns were also visualised in the form of HD-sEMG maps. This section describes these procedures.

3.6.1 MAE task maps

Another qualitative measure of the distribution of activity for the different tasks was finding the Most Active Electrode (MAE) for each task map. This was simply calculated by finding the pixel with the highest RMS value in the task map. The MAE was visualised using task-specific maps where the value of each pixel represented the number of subjects for which that electrode was the MAE of the task.

3.6.2 Repetition COG and task HD-sEMG map calculation

The lateral COG of each individual repetition for all tasks of the pattern measurements was computed for visual inspection and statistical analysis. To avoid artefacts at the beginning and the end of the contraction the first and last 15% of each repetition were discarded. The RMS of the remaining 70% of the repetition was then formed into a repetition map as described in Section 3.3.1. These COGs of these repetitions maps were calculated for comparison and use in the statistical analysis as described in Section 3.3.2.

For each task, the task map was then formed and visualised as the average of all repetition maps. The COG of the task map was also calculated for use in the data visualisation.

To allow for comparison between subjects the distance between the task-specific COG and the MVC COG in centimetres, called the normalized COG in the results. These quantities were calculated as

$$NCOG_{lat} = \frac{w(COG_{lat} - MVC_{lat})}{c-1}, NCOG_{long} = \frac{h(COG_{long} - MVC_{long})}{r-1}$$

Here MVC_{lat} and MVC_{long} is the lateral and longitudinal COG of the MVC HD-sEMG map for each subject. w is the width, h the height, c the number of columns and r the number of rows of the electrode matrix. The COG of the MVC was calculated using only the innermost 70% of the contraction data as for the other tasks.

Figure 14 illustrates how the normalized COG is calculated. The regular COG is defined using its row and column position in the HD-sEMG map. The normalized COG is normalized using the factors $w/(c-1)$ and $h/(r-1)$ to obtain distances in centimetres, giving a measure that is comparable between subjects. The MVC COG was used as a reference to account for differences in anatomy and electrode matrix placement during the comparison.

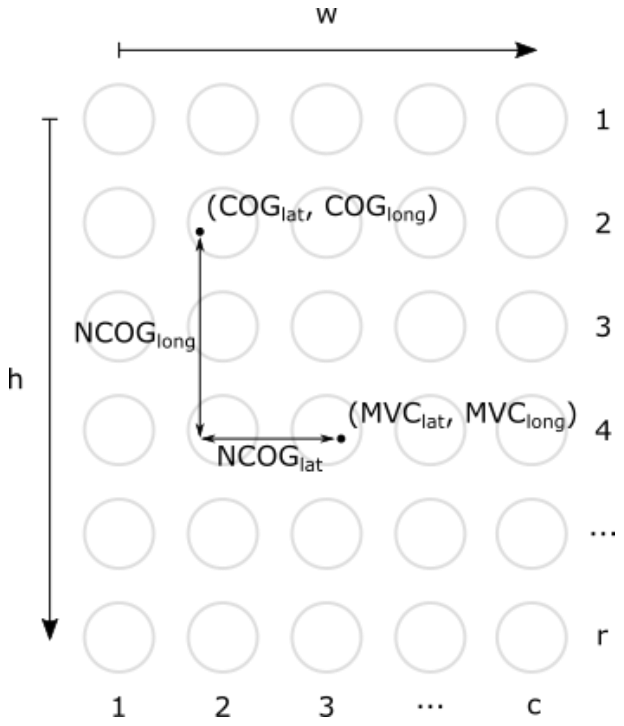

Figure 14: An illustration of how the normalized COG is calculated as the distance between the COG of the time window and the COG calculated from the MVC HD-sEMG map. The normalized COG is normalized to be given in centimeters.

3.6.3 Cluster analysis

A cluster analysis was performed on the normalised COGs to determine whether any patterns could be found for individual subjects as well as between subjects. The two main metrics of the cluster analysis was the Separability Index (SI) as suggested by Niclas Nilsson [30] to measure the separability of the tasks and the Standard Distance Deviation (SDD) to measure the clustering of the tasks.

The SI was based on the Bhattacharyya distance which is a measure of the distance between two statistical distributions. The Bhattacharyya distance was well suited for this project due to taking both distance and similarity of covariance into account, requiring few assumptions about the data. For each task, the Bhattacharyya distance to all other tasks was computed. The minimum of these distances then formed the SI, giving a measure of the separability of the task. An average of all the SI:s was also computed to give a measure of the average separability of the tasks for each subject. This metric was used to compare the separability of individual subjects and when considering all subjects combined. Both the Bhattacharyya distances and SI:s were calculated using the appropriate functions developed by Niclas Nilsson integrated in BioPatRec.

The task-specific SDD was computed as

$$SDD_t = \frac{1}{N-2}\sum_{n=0}^{N}\sqrt{(NCOG_{t,lat}(n) - \overline{NCOG_{t,lat}})^2 + (NCOG_{t,long}(n) - \overline{NCOG_{t,long}})^2}$$

where $NCOG_{t,lat}$ and $NCOG_{t,long}$ are the latitudinal and longitudinal COGs calculated for the task and $\overline{NCOG_{t,lat}}$ and $\overline{NCOG_{t,long}}$ are their respective averages. N is the number of

COGs calculated for the task. The normalization by $^{1}/_{N\,-\,2}$ is used to produce an unbiased estimate of the SDD. The SDD can be viewed as a two-dimensional standard deviation measuring the standard Euclidian distance from the mean of the COG distribution, and is used to give a measure of the clustering of the COGs. As for the SI, an average of all the SDD:s was also computed to compare the clustering of the tasks for individual subjects and when considering all subjects combined.

4 Results

In this chapter, the qualitative and quantitative results of the study are presented in form of HD-sEMG maps, task-wise and subject-wise COG distributions and a statistical analysis of the lateral COG. The Fitts's law test results are also presented to evaluate the results of the biofeedback training sessions.

4.1 Subject parameters

Table 3 shows a summary of the data gathered from the subject questionnaire as well as the measurements of the arm and electrode matrix. All subjects were right handed. Only Subject 3 had any previous EMG experience.

Table 3: Parameters gathered from the test subjects. 'c' indicates the arm circumference, 'l' the upper arm length, 'w' the width of the electrode matrix and 'h' the height of the electrode matrix. All lengths are given in centimetres.

	Gender	**Age**	**Height**	**Regular upper body exercise**	**c**	**l**	**w**	**h**
Subject 1	Male	64	176	No	30.5	31	8	9.5
Subject 2	Female	25	163	1 time/week	30	32	8.5	9
Subject 3	Male	25	170	No	25.5	34	8.25	9.5
Subject 4	Female	24	163	No	26.5	28.5	7.95	9.5
Subject 5	Male	23	180	3-4 times/week	33	36	8.25	9.5
Subject 6	Female	23	172	No	25.5	31.5	8.25	9.5
Subject 7	Male	59	174	No	37	35.5	8	9.5
Subject 8	Female	54	164	No	31.5	32.5	8	9.5

4.2 Task-specific HD-EMG and MAE maps

Figure 15 to Figure 22 show the computed task-specific HD-sEMG maps and Most Active Electrode (MAE) maps for all subjects. The maps for the tasks open hand, close hand, extend hand, flex hand, pronation and extend elbow show what primarily seems to be cross-talk from other muscles as the activity is concentrated along the edges of the matrix, while supination and flex elbow tasks show large activation of primarily the BB. Note how the activity seems concentrated to a few electrodes for the tasks where the BB is primarily activated. The HD-sEMG maps are presented from Subject 1 to Subject 8, in order from left to right with Subject 1 being in the top left.

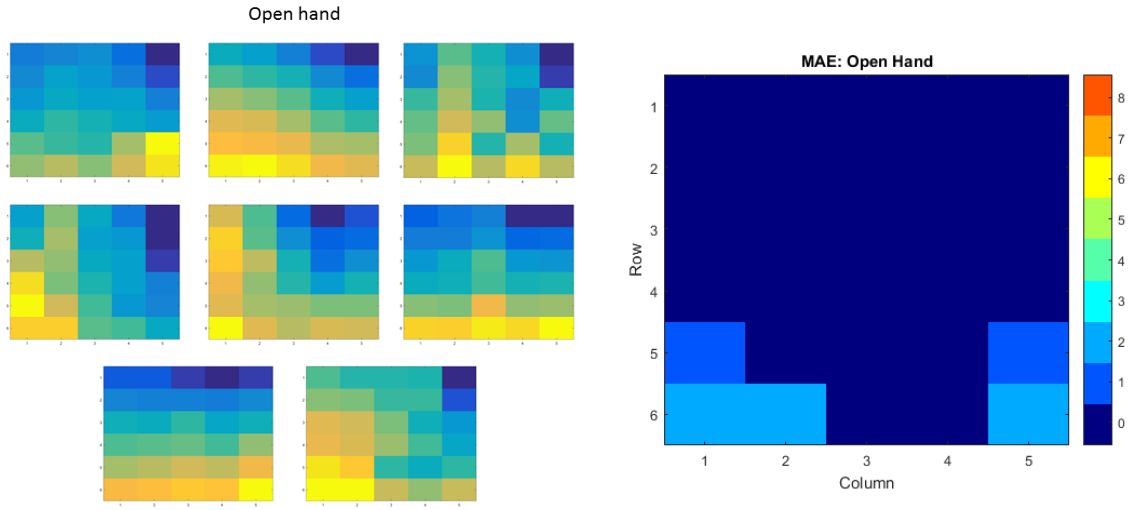

Figure 15: HD-sEMG and MAE maps for the "Open hand" task. The HD-sEMG maps are averaged over all repetitions for each subject. The colour of each pixel of the MAE map indicate the number of subjects for which that electrode was the MAE.

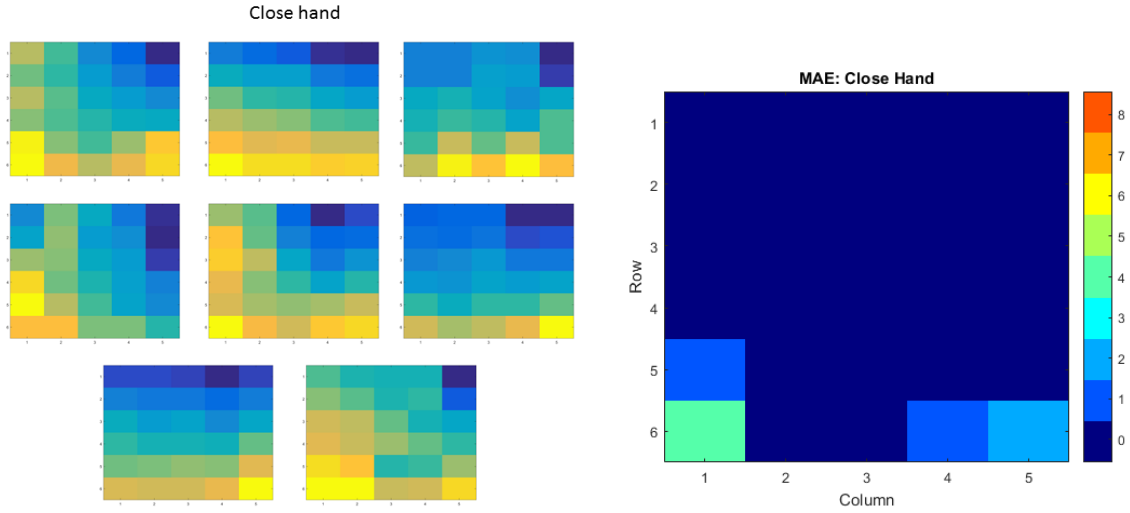

Figure 16: HD-sEMG and MAE maps for the "Close hand" task. The HD-sEMG maps are averaged over all repetitions for each subject. The colour of each pixel of the MAE map indicate the number of subjects for which that electrode was the MAE.

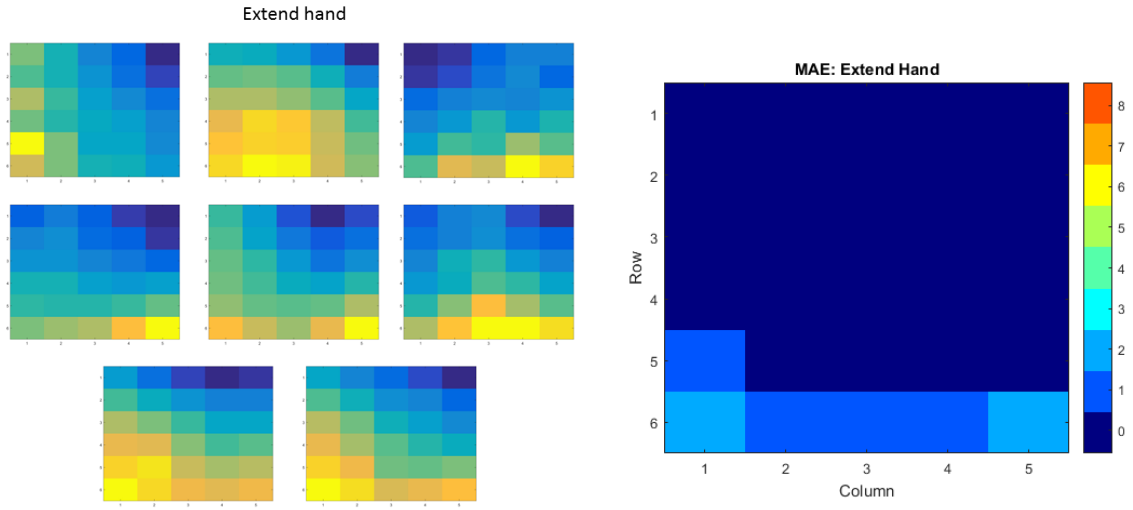

Figure 17: HD-sEMG and MAE maps for the "Extend hand" task. The HD-sEMG maps are averaged over all repetitions for each subject. The colour of each pixel of the MAE map indicate the number of subjects for which that electrode was the MAE.

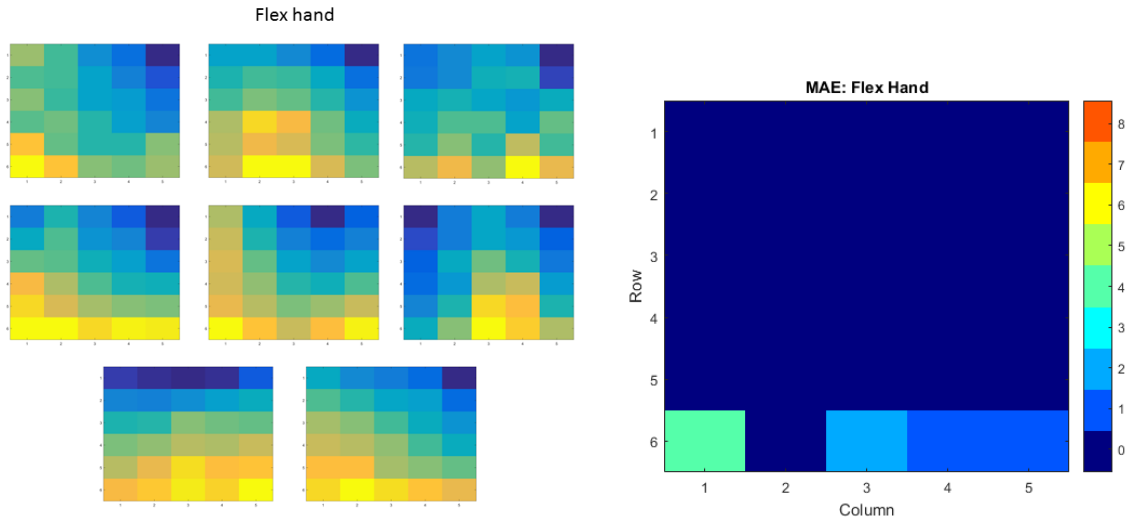

Figure 18: HD-sEMG and MAE maps for the "Flex hand" task. The HD-sEMG maps are averaged over all repetitions for each subject. The colour of each pixel of the MAE map indicate the number of subjects for which that electrode was the MAE.

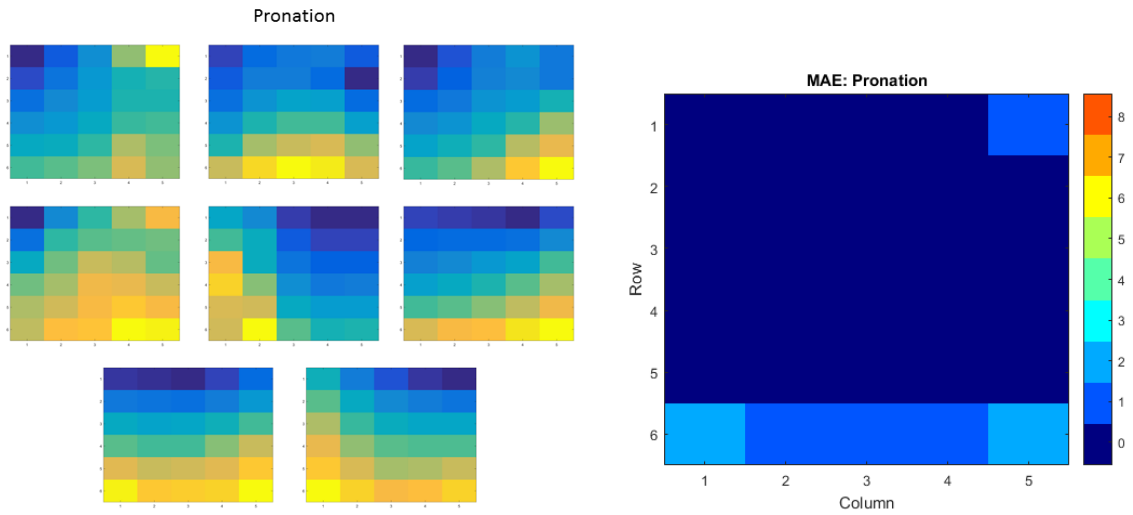

Figure 19: HD-sEMG and MAE maps for the "Pronation" task. The HD-sEMG maps are averaged over all repetitions for each subject. The colour of each pixel of the MAE map indicate the number of subjects for which that electrode was the MAE.

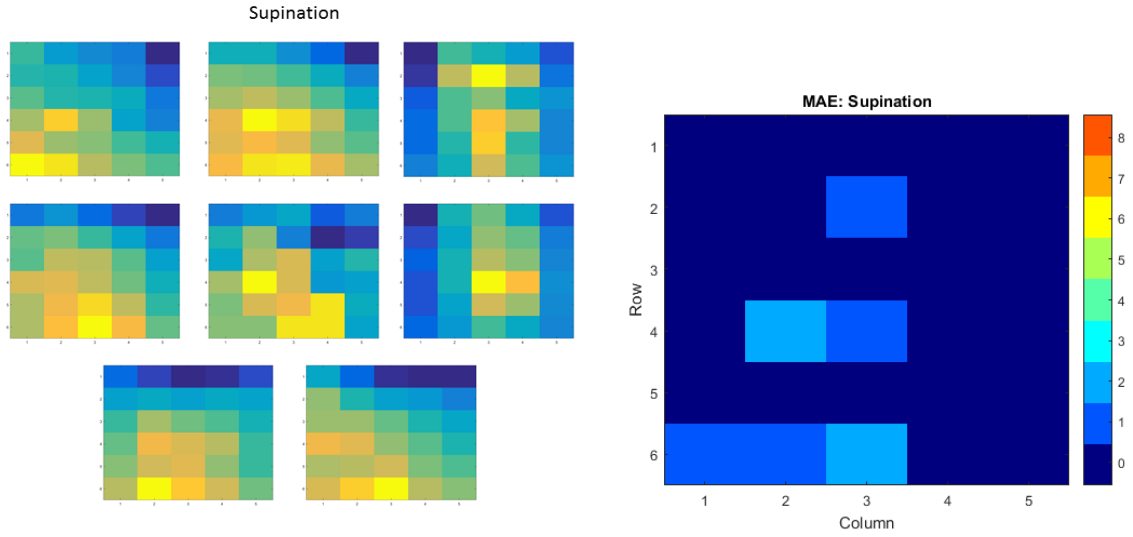

Figure 20: HD-sEMG and MAE maps for the "Supination" task. The HD-sEMG maps are averaged over all repetitions for each subject. The colour of each pixel of the MAE map indicate the number of subjects for which that electrode was the MAE.

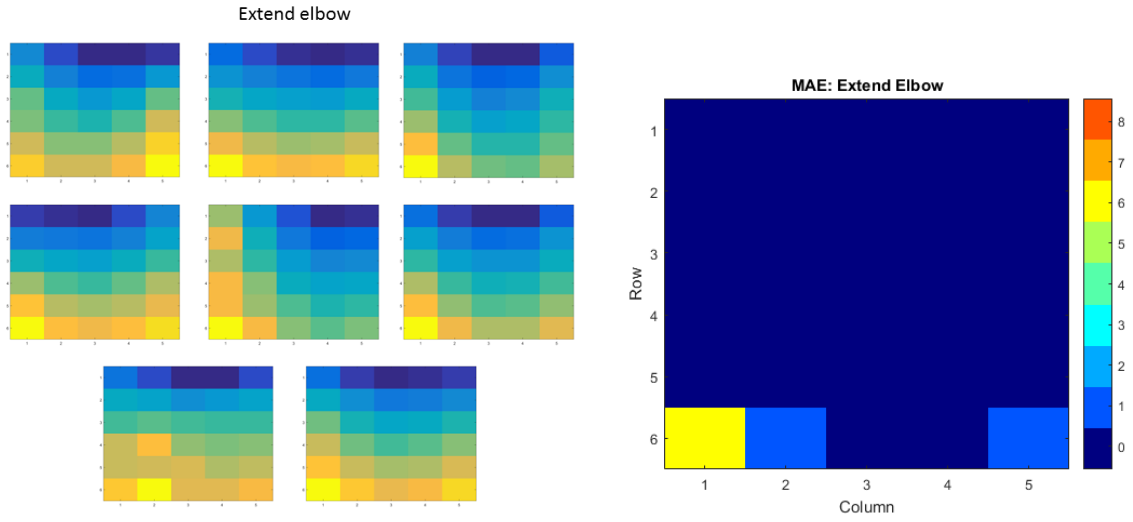

Figure 21: HD-sEMG and MAE maps for the "Extend elbow" task. The HD-sEMG maps are averaged over all repetitions for each subject. The colour of each pixel of the MAE map indicate the number of subjects for which that electrode was the MAE.

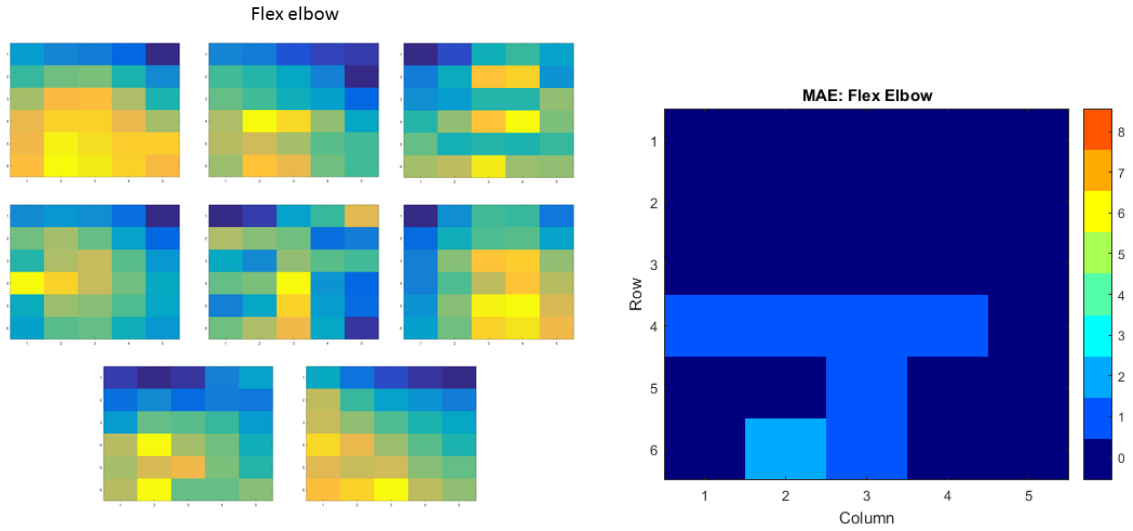

Figure 22: HD-sEMG and MAE maps for the "Flex elbow" task. The HD-sEMG maps are averaged over all repetitions for each subject. The colour of each pixel of the MAE map indicate the number of subjects for which that electrode was the MAE.

4.3 Subject-wise normalized COG

Figure 23 to Figure 30 show the normalized COGs grouped per subject. Each symbol represents the normalized COG of an individual time window. Note how most subjects display at least some grouping of the COGs for each task. Also note the small scale of the axes, indicating only small variations in the COG for the different tasks.

Table 4 to Table 11 show the cluster analysis results for each subject. The leftmost parts of the tables show the Bhattacharyya distance between movements, while the rightmost two columns show the SI and SDD for each movement. Green cells indicate a result within the top 25% of the respective metric (above the 75th percentile for the Bhattacharyya distances and the SI, below the 25th percentile for the SDD) while red cells indicate a result within the bottom 25% of the respective metric (under the 23th percentile for the Bhattacharyya distances and the SI, above the 75th percentile for the SDD).

The results seem to show some variation in the separability for each subject, although all subjects display at least some amount of separation between movements. The movement with highest SI was pronation for two subjects, flex hand for one subject, extend elbow for three subjects and flex elbow for two subjects, showing that no movement seems much more separable than the others.

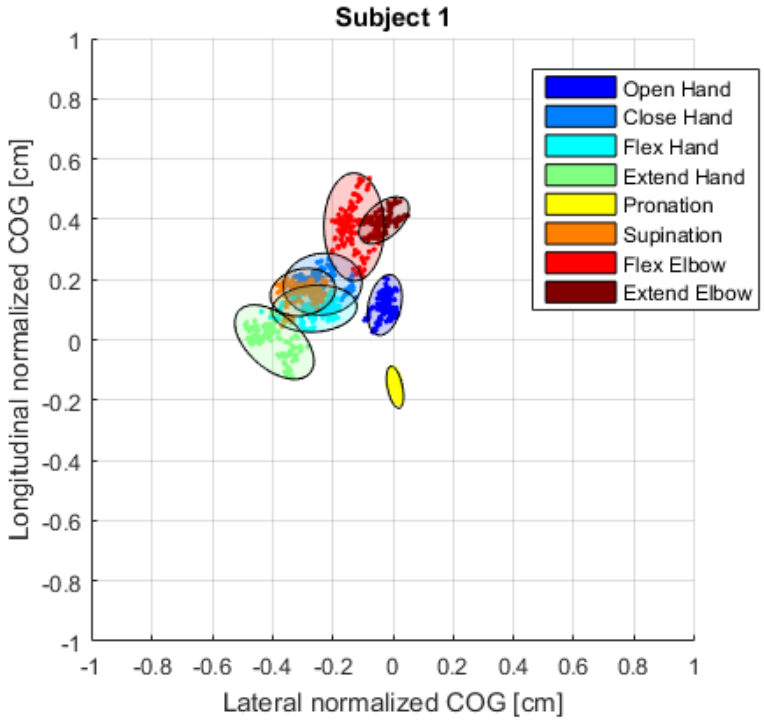

Figure 23: The COG distributions of the movements for Subject 1. The markers indicate the computed COGs for individual time windows, while the ellipses denote the 95% confidence interval of the distribution computed from the covariance of the COG distribution.

Table 4: The Bhattacharyya distances between movements as well as the Separability Index (SI) and Standard Distance Deviation (SDD) for each movement for Subject 1. Green cells indicate results above the 75th percentile of the metric while red cells indicate results below the 25th percentile.

Bhattacharyya distance										
	Open Hand	**Close Hand**	**Flex Hand**	**Extend Hand**	**Pronation**	**Supination**	**Flex Elbow**	**Extend Elbow**	**SI**	**SDD**
Open Hand	0	1,94	1,89	3,67	2,87	2,85	1,95	2,90	1,89	0,043
Close Hand		0	0,76	2,06	4,04	0,51	1,35	2,34	0,51	0,063
Flex Hand			0	1,45	3,84	0,66	1,93	3,38	0,66	0,059
Extend Hand				0	3,71	1,76	3,30	5,01	1,45	0,070
Pronation					0	5,05	3,71	6,84	2,87	0,028
Supination						0	1,92	3,09	0,51	0,050
Flex Elbow							0	1,01	1,01	0,074
Extend Elbow								0	1,01	0,043
								Average	1,24	0,054

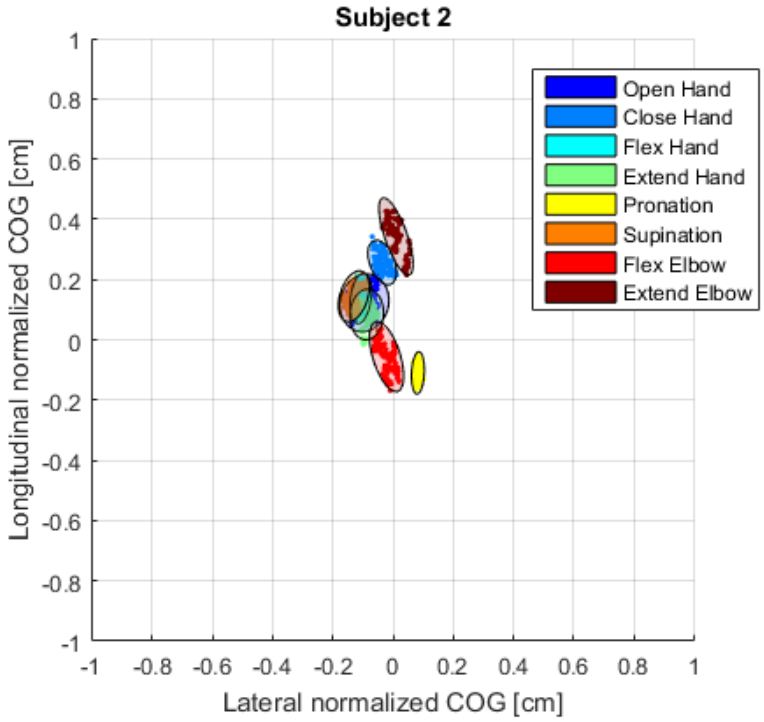

Figure 24: The COG distributions of the movements for Subject 2. The markers indicate the computed COGs for individual time windows, while the ellipses denote the 95% confidence interval of the distribution computed from the covariance of the COG distribution.

Table 5: The Bhattacharyya distances between movements as well as the Separability Index (SI) and Standard Distance Deviation (SDD) for each movement for Subject 2. Green cells indicate results above the 75th percentile of the metric while red cells indicate results below the 25th percentile.

Bhattacharyya distance										
	Open Hand	**Close Hand**	**Flex Hand**	**Extend Hand**	**Pronation**	**Supination**	**Flex Elbow**	**Extend Elbow**	**SI**	**SDD**
Open Hand	0	1,60	0,44	0,40	3,70	0,56	1,58	2,51	0,40	0,049
Close Hand		0	2,05	2,18	4,73	2,01	3,04	1,67	1,60	0,033
Flex Hand			0	0,71	6,88	0,49	1,99	3,56	0,44	0,033
Extend Hand				0	4,22	1,01	1,36	3,28	0,40	0,037
Pronation					0	6,37	2,17	3,87	2,17	0,028
Supination						0	2,22	3,28	0,49	0,038
Flex Elbow							0	4,06	1,36	0,048
Extend Elbow								0	1,67	0,049
								Average	1,07	0,039

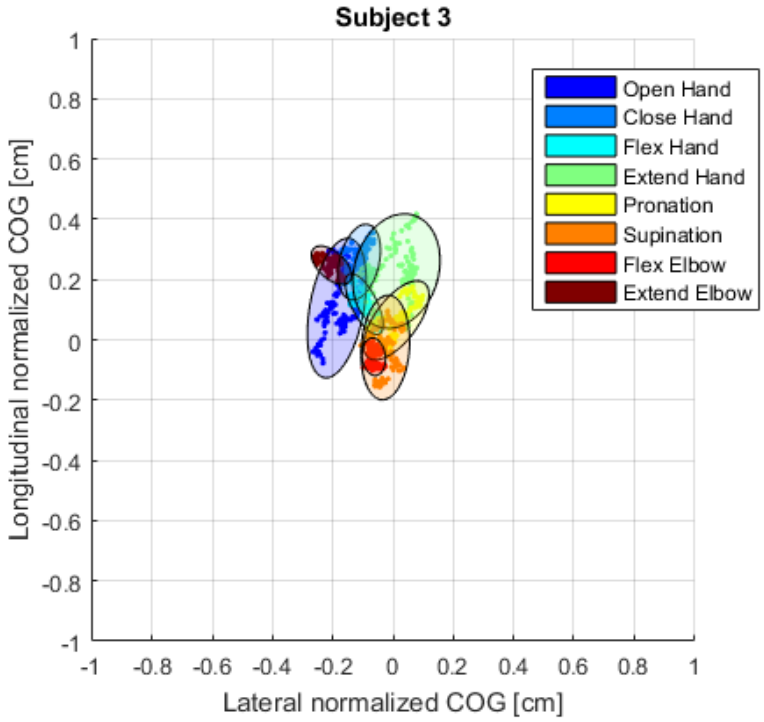

Figure 25: The COG distributions of the movements for Subject 3. The markers indicate the computed COGs for individual time windows, while the ellipses denote the 95% confidence interval of the distribution computed from the covariance of the COG distribution.

Table 6: The Bhattacharyya distances between movements as well as the Separability Index (SI) and Standard Distance Deviation (SDD) for each movement for Subject 3. Green cells indicate results above the 75th percentile of the metric while red cells indicate results below the 25th percentile.

Bhattacharyya distance										
	Open Hand	**Close Hand**	**Flex Hand**	**Extend Hand**	**Pronation**	**Supination**	**Flex Elbow**	**Extend Elbow**	**SI**	**SDD**
Open Hand	0	0,92	1,10	1,37	1,95	1,82	2,05	1,02	0,92	0,089
Close Hand		0	1,11	1,05	2,45	2,06	3,05	1,22	0,92	0,053
Flex Hand			0	1,17	1,32	1,20	1,85	1,54	1,10	0,041
Extend Hand				0	0,95	1,20	1,90	1,77	0,95	0,089
Pronation					0	0,58	1,17	3,22	0,58	0,063
Supination						0	0,77	2,73	0,58	0,072
Flex Elbow							0	4,19	0,77	0,028
Extend Elbow								0	1,02	0,035
								Average	0,85	0,059

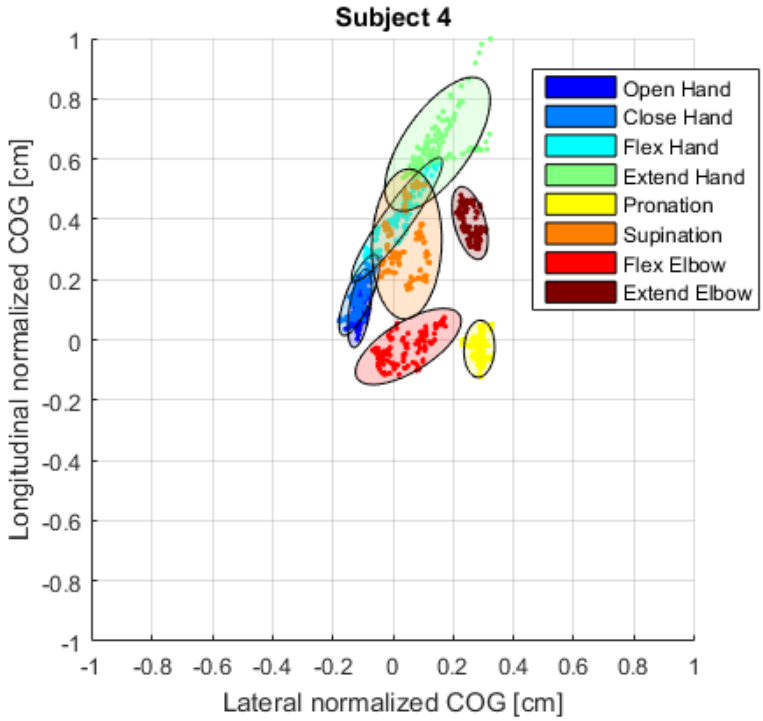

Figure 26: The COG distributions of the movements for Subject 4. The markers indicate the computed COGs for individual time windows, while the ellipses denote the 95% confidence interval of the distribution computed from the covariance of the COG distribution.

Table 7: The Bhattacharyya distances between movements as well as the Separability Index (SI) and Standard Distance Deviation (SDD) for each movement for Subject 4. Green cells indicate results above the 75th percentile of the metric while red cells indicate results below the 25th percentile.

Bhattacharyya distance										
	Open Hand	**Close Hand**	**Flex Hand**	**Extend Hand**	**Pronation**	**Supination**	**Flex Elbow**	**Extend Elbow**	**SI**	**SDD**
Open Hand	0	0,45	1,63	2,65	8,09	1,79	2,09	6,62	0,45	0,050
Close Hand		0	1,31	2,39	7,56	1,57	2,54	5,03	0,45	0,054
Flex Hand			0	1,06	7,06	0,76	3,66	2,53	0,76	0,085
Extend Hand				0	5,05	1,23	3,80	2,03	1,06	0,096
Pronation					0	2,92	1,94	3,31	1,94	0,039
Supination						0	1,60	2,03	0,76	0,104
Flex Elbow							0	2,92	1,60	0,083
Extend Elbow								0	2,03	0,052
								Average	1,13	0,070

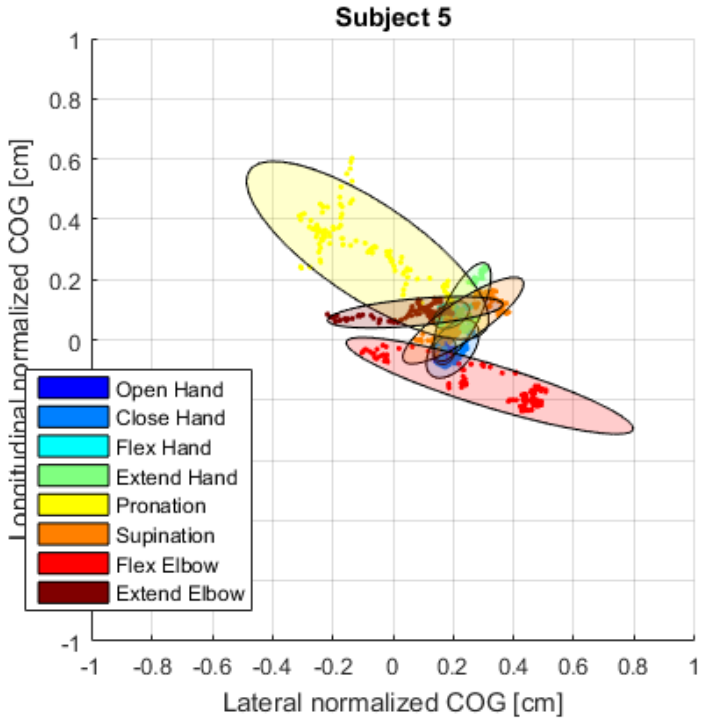

Figure 27: The COG distributions of the movements for Subject 5. The markers indicate the computed COGs for individual time windows, while the ellipses denote the 95% confidence interval of the distribution computed from the covariance of the COG distribution.

Table 8: The Bhattacharyya distances between movements as well as the Separability Index (SI) and Standard Distance Deviation (SDD) for each movement for Subject 5. Green cells indicate results above the 75th percentile of the metric while red cells indicate results below the 25th percentile.

Bhattacharyya distance										
	Open Hand	**Close Hand**	**Flex Hand**	**Extend Hand**	**Pronation**	**Supination**	**Flex Elbow**	**Extend Elbow**	**SI**	**SDD**
Open Hand	0	0,58	2,23	1,09	1,77	1,17	1,42	2,73	0,58	0,022
Close Hand		0	1,50	0,83	1,49	0,87	1,17	1,80	0,58	0,051
Flex Hand			0	0,71	1,35	0,85	2,76	0,92	0,71	0,027
Extend Hand				0	1,23	0,52	1,65	1,04	0,52	0,065
Pronation					0	1,26	1,82	1,14	1,14	0,187
Supination						0	1,51	1,06	0,52	0,095
Flex Elbow							0	2,02	1,17	0,182
Extend Elbow								0	0,92	0,101
								Average	0,77	0,091

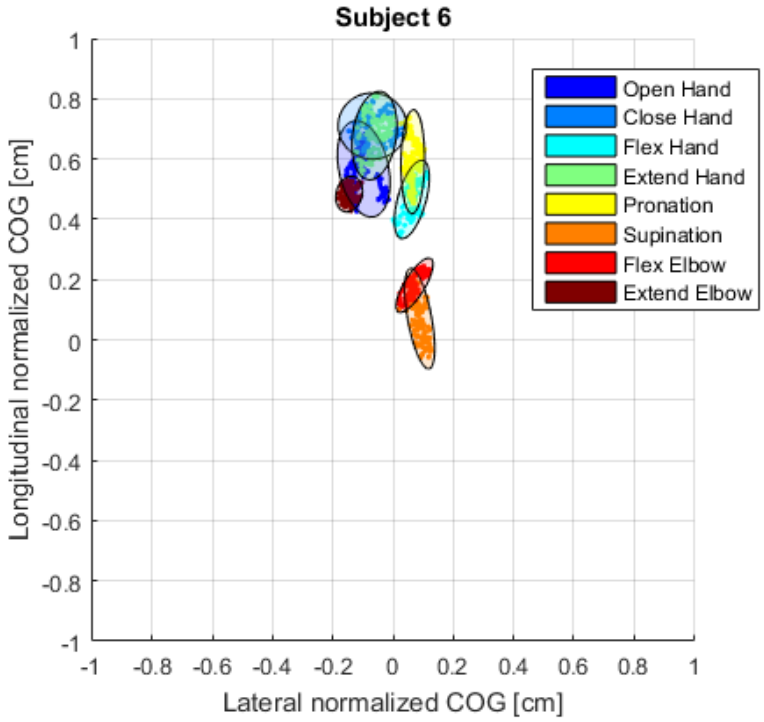

Figure 28: The COG distributions of the movements for Subject 6. The markers indicate the computed COGs for individual time windows, while the ellipses denote the 95% confidence interval of the distribution computed from the covariance of the COG distribution.

Table 9: The Bhattacharyya distances between movements as well as the Separability Index (SI) and Standard Distance Deviation (SDD) for each movement for Subject 6. Green cells indicate results above the 75th percentile of the metric while red cells indicate results below the 25th percentile.

Bhattacharyya distance										
	Open Hand	**Close Hand**	**Flex Hand**	**Extend Hand**	**Pronation**	**Supination**	**Flex Elbow**	**Extend Elbow**	**SI**	**SDD**
Open Hand	0	0,97	1,96	0,74	2,13	2,94	3,25	1,08	0,74	0,068
Close Hand		0	2,38	0,31	1,59	3,98	5,14	2,36	0,31	0,061
Flex Hand			0	2,55	0,76	2,31	2,92	3,94	0,76	0,052
Extend Hand				0	1,97	3,70	4,85	1,78	0,31	0,060
Pronation					0	2,65	2,78	4,36	0,76	0,063
Supination						0	0,96	4,48	0,96	0,064
Flex Elbow							0	7,48	0,96	0,041
Extend Elbow								0	1,08	0,028
								Average	0,73	0,055

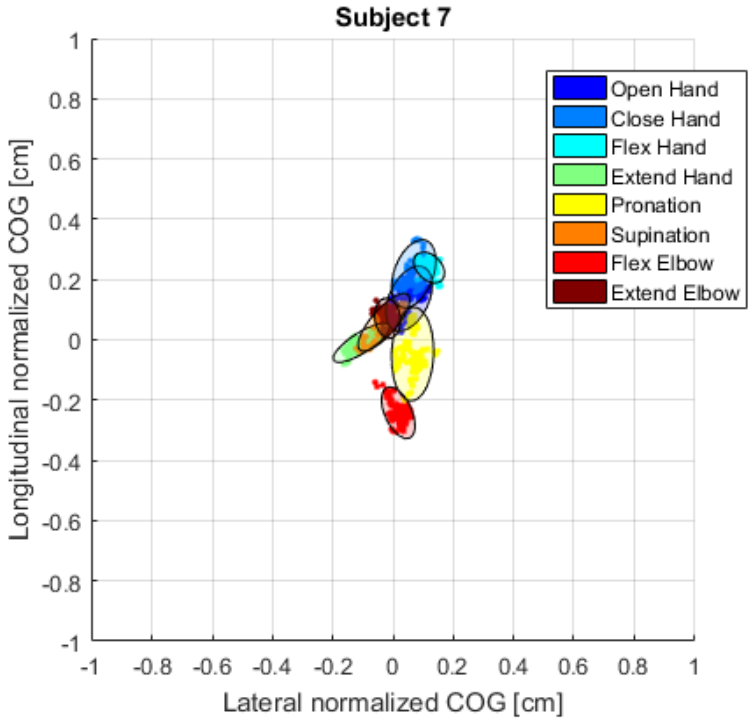

Figure 29: The COG distributions of the movements for Subject 7. The markers indicate the computed COGs for individual time windows, while the ellipses denote the 95% confidence interval of the distribution computed from the covariance of the COG distribution.

Table 10: The Bhattacharyya distances between movements as well as the Separability Index (SI) and Standard Distance Deviation (SDD) for each movement for Subject 7. Green cells indicate results above the 75th percentile of the metric while red cells indicate results below the 25th percentile.

Bhattacharyya distance										
	Open Hand	**Close Hand**	**Flex Hand**	**Extend Hand**	**Pronation**	**Supination**	**Flex Elbow**	**Extend Elbow**	**SI**	**SDD**
Open Hand	0	0,62	1,30	1,74	1,24	0,91	3,36	1,08	0,62	0,049
Close Hand		0	0,82	2,29	1,70	1,37	3,99	1,66	0,62	0,050
Flex Hand			0	3,84	2,33	2,28	7,59	4,01	0,82	0,026
Extend Hand				0	2,01	0,78	3,32	1,29	0,78	0,042
Pronation					0	1,60	1,58	1,55	1,24	0,061
Supination						0	3,25	0,45	0,45	0,044
Flex Elbow							0	3,58	1,58	0,036
Extend Elbow								0	0,45	0,029
								Average	0,82	0,042

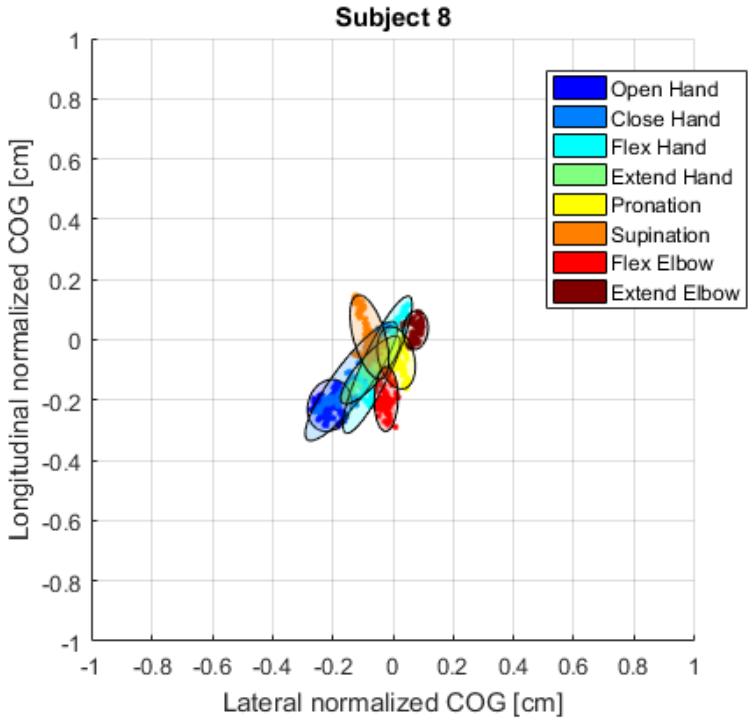

Figure 30: The COG distributions of the movements for Subject 8. The markers indicate the computed COGs for individual time windows, while the ellipses denote the 95% confidence interval of the distribution computed from the covariance of the COG distribution.

Table 11: The Bhattacharyya distances between movements as well as the Separability Index (SI) and Standard Distance Deviation (SDD) for each movement for Subject 8. Green cells indicate results above the 75th percentile of the metric while red cells indicate results below the 25th percentile.

Bhattacharyya distance										
	Open Hand	**Close Hand**	**Flex Hand**	**Extend Hand**	**Pronation**	**Supination**	**Flex Elbow**	**Extend Elbow**	**SI**	**SDD**
Open Hand	0	0,69	1,57	1,39	3,23	2,71	2,77	4,74	0,69	0,042
Close Hand		0	0,77	0,59	1,29	0,97	1,84	1,83	0,59	0,084
Flex Hand			0	0,44	0,86	0,91	1,31	1,54	0,44	0,093
Extend Hand				0	0,99	0,96	1,52	1,73	0,44	0,052
Pronation					0	1,18	1,33	1,52	0,86	0,045
Supination						0	1,48	2,71	0,91	0,053
Flex Elbow							0	2,93	1,31	0,040
Extend Elbow								0	1,52	0,028
								Average	0,84	0,055

Figure 31 shows the COG distribution when combining the COGs from all subjects, with and without the 95% confidence intervals shown for increased visibility. Note the wider COG spread for each task when compared to the individual subjects shown in Figure 23 to Figure 30, indicating that the patterns are not consistent between subjects. This is reflected in Table 12 which shows lower Bhattacharyya distances and SI:s as well as higher SDD:s than most individual subjects, indicating a lower amount of separability and clustering of the movements.

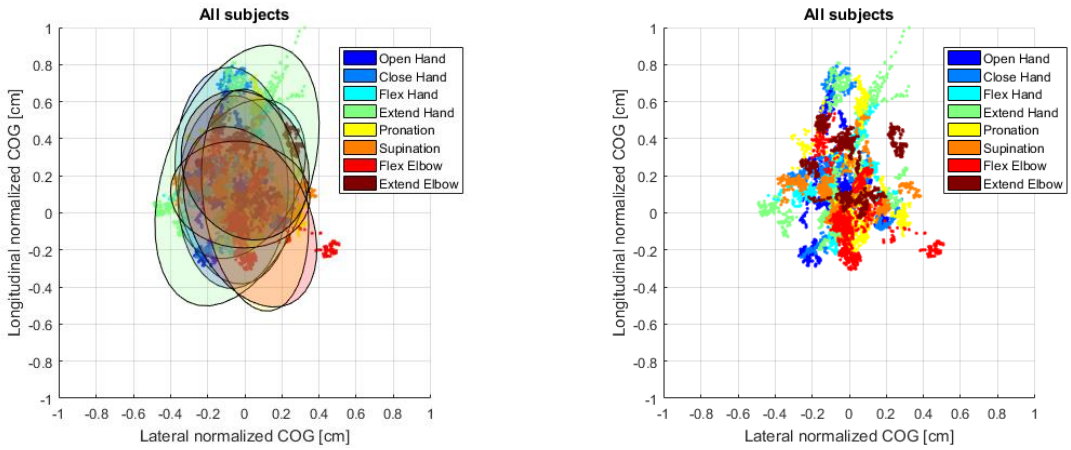

Figure 31: The COG distributions of the movements for all subjects combined. The markers indicate the computed COGs for individual time windows. The left plot shows ellipses denoting the 95% confidence interval of the distribution computed from the covariance of the COG distribution. The right figure shows the COG distribution without the confidence intervals overlaid.

Table 12: The Bhattacharyya distances between movements as well as the Separability Index (SI) and Standard Distance Deviation (SDD) for each movement for all subjects combined. Green cells indicate results above the 75th percentile of the metric while red cells indicate results below the 25th percentile.

Bhattacharyya distance										
	Open Hand	**Close Hand**	**Flex Hand**	**Extend Hand**	**Pronation**	**Supination**	**Flex Elbow**	**Extend Elbow**	**SI**	**SDD**
Open Hand	0	0,13	0,20	0,25	0,33	0,29	0,31	0,33	0,13	0,195
Close Hand		0	0,21	0,20	0,31	0,36	0,37	0,23	0,13	0,222
Flex Hand			0	0,24	0,35	0,27	0,43	0,19	0,19	0,207
Extend Hand				0	0,39	0,44	0,46	0,31	0,20	0,306
Pronation					0	0,39	0,21	0,36	0,21	0,229
Supination						0	0,34	0,40	0,27	0,169
Flex Elbow							0	0,52	0,21	0,207
Extend Elbow								0	0,19	0,207
								Average	0,19	0,218

Figure 32 shows a box plot summarizing the SI:s for individual subjects and all subjects combined. The average SI for individual subjects is 0.9313, while the average SI for all subjects combined is 0.1909, 79.5% less than for individual subjects.

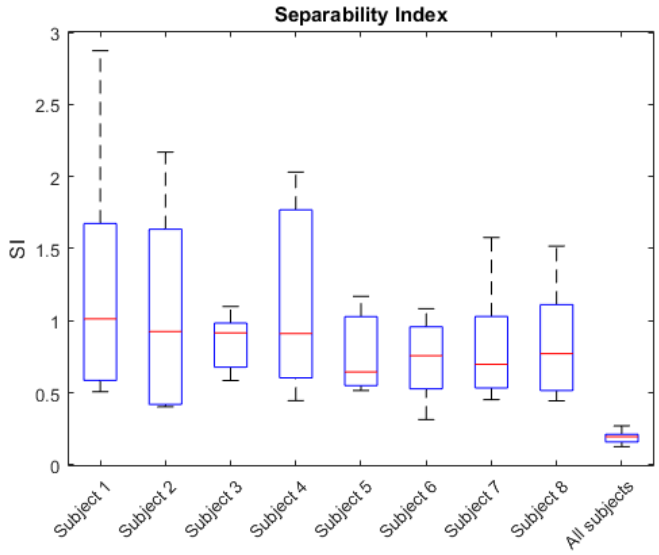

Figure 32: Box plot of the Separability Index spread for individual subjects and all subjects combined.

Figure 33 instead shows a box plot summarizing the SDD:s for individual subjects and all subjects combined. The average SDD for individual subjects is 0.0564, while the average SDD for all subjects combined is 0.2164, 284% more than for individual subjects

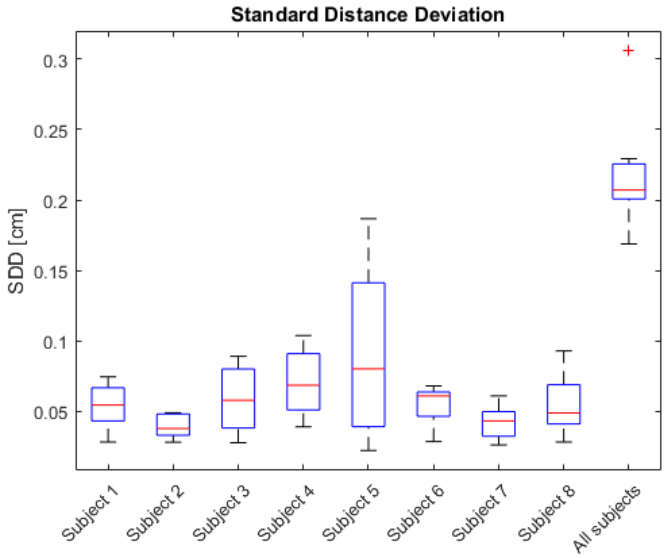

Figure 33: Box plot of the Standard Distance Deviation spread for individual subjects and all subjects combined.

4.4 Fitts's law results

Figure 34 to Figure 37 show the metrics gathered during the Fitts's law tests during the biofeedback training. The thick red lines indicate the averaged metrics for all subjects. Efficiency, overshoot and throughput were only calculated for successfully completed repetitions of the test. Note that in some cases technical or user issues prevented one or more tests from taking place. In these cases, it was deemed more efficient to skip the tests to focus on resolving the issues before resuming the training.

Figure 34 shows the Completion Rate (CR) metric, indicating the percentage of completed repetitions, for non-fixated and fixated arm. In both cases the CR went up during the training session. For the session with non-fixated arm most of the improvement happened between test one and two, with in fact a slight decrease in average CR between test two and three. For the session with fixated arm most of the improvement happened between test two and three. The completion rate was on average lower for the session with fixated arm, suggesting an increased level of challenge for that session.

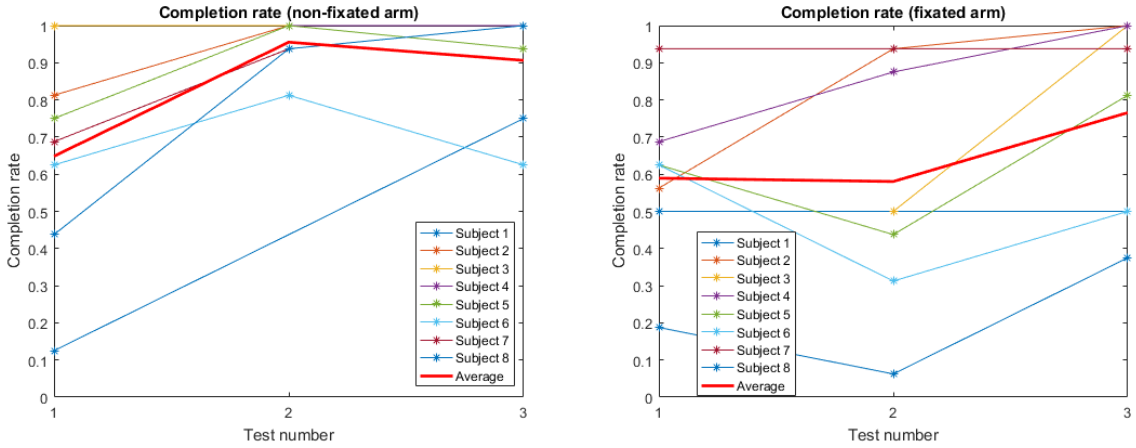

Figure 34: The Completion Rate metric, indicating the percentage of completed repetitions, for non-fixated and fixated arm.

Figure 35 shows the Overshoot (O) metric, indicating the average number of the times the target was acquired and then lost for each repetition, giving a measure of the level of fine control of the GUI. The metric stays relatively constant throughout both sessions.

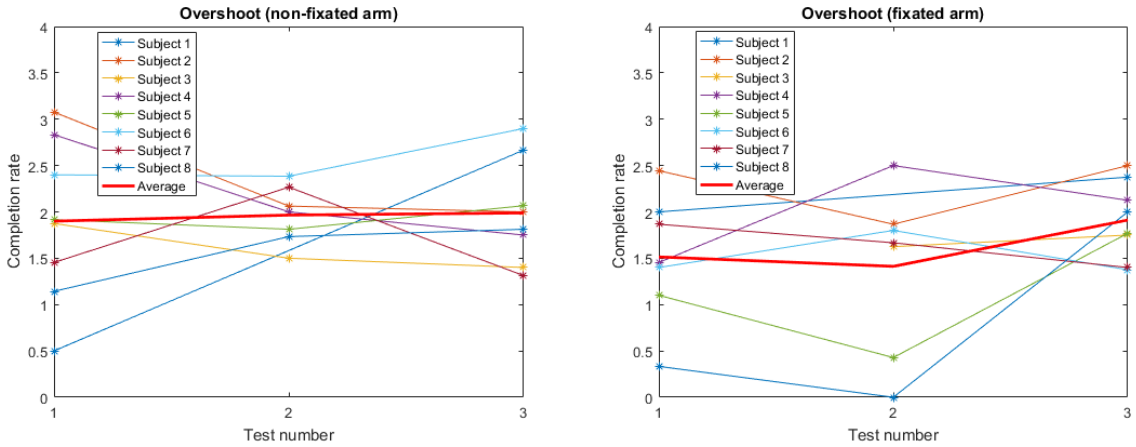

Figure 35: The Overshoot metric, indicating the average number of times the target was acquired and then lost for each repetition, for non-fixated and fixated arm.

Figure 36 shows the Efficiency metric, indicating the ratio between the length of the optimal path and the taken path to the target, giving a measure of the overall precision of the control of the GUI. On average it stays relatively constant during both training sessions.

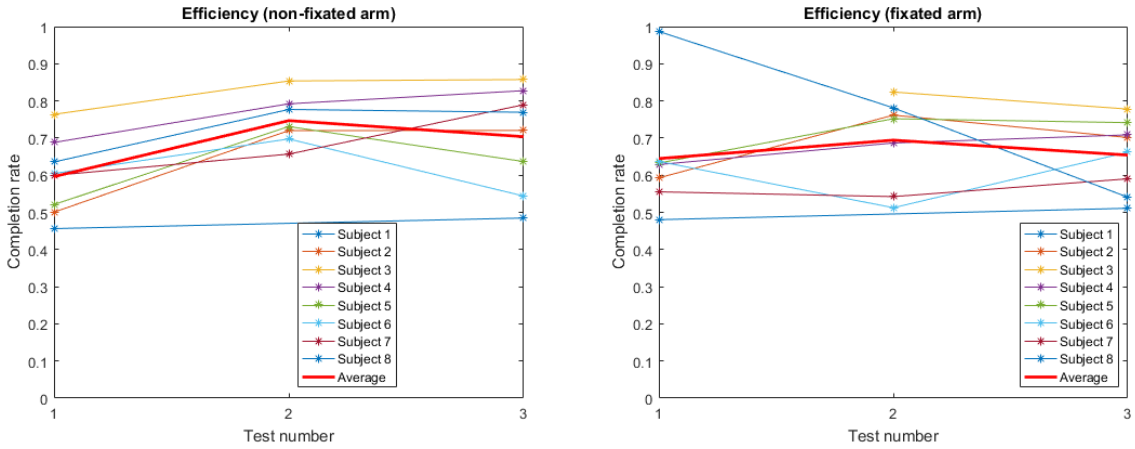

Figure 36: The Efficiency metric, indicating the ratio between the length of the optimal path and the taken path to the target, for non-fixated and fixated arm.

Figure 37 shows the Throughput metric, computed as a function of clear time and Index of Difficulty for each repetition as described in Section 2.8. The Throughput gives a general index of performance for each subject. The Throughput sees an increase on average for the both sessions, although a slight one for the session with fixated arm.

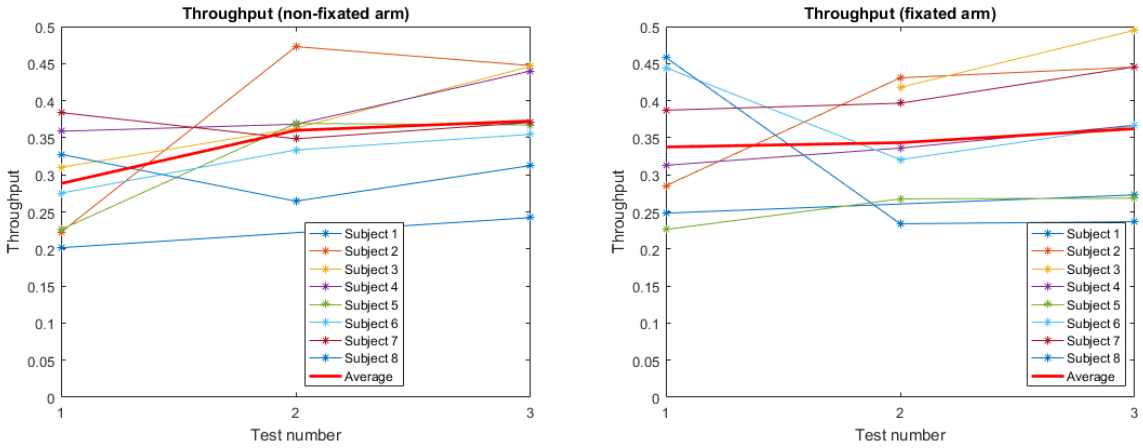

Figure 37: The Throughput metric, computed as a function of clear time and Index of Difficulty for each repetition, for non-fixated and fixated arm.

Table 13 shows a summary of the average change of the metrics during the biofeedback training session with non-fixated arm. All metrics showed an improvement except overshoot which showed a slight increase. This indicates that the subjects on average achieved an improved control over the Biofeedback GUI.

Table 13: Summary of the Fitts's law metrics collected during biofeedback training with non-fixated arm

	Average, session 1	Average, session 3	Difference
Completion rate	0.6484	0.9063	0.2579
Throughput	0.2883	0.3726	0.0843
Efficiency	0.5962	0.7037	0.1075
Overshoot	1.8999	1.9885	0.0886

Table 14 shows instead a summary of the average change of the metrics during the biofeedback training session with fixated arm. As for the session with non-fixated arm, all metrics except overshoot saw an improvement on average. Note the lower average completion rate, indicating that the tests with fixating arm were harder to complete. The higher throughput and efficiency and lower overshoot can be a result of the fact that only completed repetitions factor into these metrics. The proportion between difficult and easier repetitions can thus be different between the two training sessions, thus making these metrics hard to compare.

Table 14: Summary of the Fitts's law metrics collected during biofeedback training with fixated arm

	Average, session 1	Average, session 3	Difference
Completion rate	0.5893	0.7656	0.1763
Throughput	0.3375	0.3622	0.0247
Efficiency	0.6448	0.6542	0.0094
Overshoot	1.5141	1.9118	0.3977

5 Discussion

This chapter discusses the results and findings of the projects and how they can be applied for future applications and work.

5.1 Limitations of the measurement methods

Even though many subjects saw substantial improvement during the biofeedback training, it is debatable whether this was due to improved differential activation. Surface EMG is prone to effects such cross-talk, shifting of the muscular bulk and skin stretching. It was also in some cases difficult to place the electrode matrix in such a way that only the BB was covered, meaning that especially corners and edges of the matrix would be covering other muscles, influencing the results. The effects of skin stretching and muscle shifting were somewhat controlled in the training session with fixated arm, although the effect of cross-talk and electrode matrix coverage of other muscles was still not fully controlled.

These effects meant that it is difficult to conclusively determine whether the improved control of the GUI was due to improved voluntary differential activation of the BB. It might as well be that the improved control was due to activation of other muscles, causing cross-talk and shifting the COG, or other involuntary compensatory strategies such as shifting the muscle under the skin or stretching the skin. To control for these effects and conclusively determine the amount of differential activation it might be necessary to use complex source separation strategies or even intramuscular electrodes.

5.2 Discussion of the pattern analysis results

As can be seen in Figure 23 to Figure 30, the COG seems to be consistent for each task for individual subjects. This indicates that there are patterns in the muscular activation of the BB during distal tasks. However, as seen in Figure 31, no clear such pattern can be found when studying the tasks for all subjects combined. Although it is up to debate whether the method used for normalising the COG is optimal, a qualitative study of the individual subject COG patterns in Figure 23 to Figure 30 suggest that it would be difficult to find any common patterns due to the major differences in the general appearance of the activation patterns.

Another thing to note is that the spread of the COG ranges over only a few centimetres, much less than the span of the BB. The reason for this is probably that the noise, which is spread evenly over the HD-sEMG maps, forces the COG to the centre of the map, as the weak signal strengths of the distal movements are on the same order of magnitude as the noise floor.

These facts suggest that the COG served the purpose of quantitatively finding patterns in muscular activation between movements well. However, other methods of analysis might be necessary to extract information to use from the activation patterns. Apart from the issue of the COG gravitating towards the centre of the map due to noise, the COG is also prone to influence from cross-talk. This means that the MAE maps as seen in Figure 15 to Figure 22 might be better suited for studying the patterns qualitatively.

5.2.1 Interpretation of the Separability Index metric

Even though the Separability Index was conceived as a measure of classification complexity of a set of movements [30] and thus could reasonably be interpreted as a measure of separation between movements, it deserves some additional thought when used in the context of this thesis. When computed from the Bhattacharyya distance, which measures differences in both variance and mean of the COG distributions, a large SI can mean that a movement differs from the other movements either by a significant difference in mean COG, a significant difference in the variance of the COG, or both. Two movements with the same mean COG can thus be separated by a large Bhattacharyya distance if the variances differ enough, even though it would be difficult to classify the movement by studying only the COG. This means that the SI should rather be thought of as a measure of differences in the COG distribution between movements, and a large average SI for a subject might not necessarily mean that the COG distributions are clearly distinguishable from each other. However, the COG only represents two features of the EMG (lateral and longitudinal COG). Even if it would be difficult to classify movements by the COG alone, it could very well be possible by considering the COG in combination with other signal features. In this way the COG could prove a valuable additional feature for classification purposes, which could be an interesting area of further research.

5.2.2 Segmentation of the high-density EMG maps

Visualisation in the form of HD-sEMG maps allows distinguishing separate activation areas, such as different muscles or compartments within a single muscle, as the activation areas yield clusters of high-intensity pixels in the HD-sEMG maps [11]. A rudimentary segmentation trial using this kind of segmentation was performed on the HD-sEMG task maps collected from this study to see whether any compartments could be discerned. The trial was performed using the built-in **watershed()** function of Matlab. However, the trial yielded no useful information, with seemingly random segmentation results which were thus not included in the study. Probable causes for this are the low resolution of the HD-sEMG maps from an image processing standpoint and that the watershed segmentation method might simply not be well suited for segmentation of HD-sEMG maps without some modification.

An interesting area for further research could be to explore the possibilities of spatial segmentation to aid in discerning muscular activation areas algorithmically. Previously used HD-sEMG segmentation methods include a method proposed by Vieira et al. based on watershed segmentation [13] and a method proposed by Rojas-Martínez et al. based on the h-dome transform [11].

5.3 Biofeedback training results discussion

Most metrics for the case with non-fixated arm, as seen in Figure 34 to Figure 37, seem to see the most improvement between the first and second test and only marginal improvement or even a slight decline between the second and third test. This suggests that

much of the improvement comes from getting used to the GUI as opposed to an increased level of differential activation.

For the metrics with fixated arm, as seen in Figure 34 to Figure 37, most of the improvement instead seems to happen between the second and third test. This is probably a result of the increased challenge of controlling the GUI with fixated arm which makes it take more experimentation for the subject to find a method that works to control it.

It should be noted that completion rates lower than 0.5 can be achieved even without proper control of the GUI, as the Fitts's law test is designed so that half of the repetitions are located on each side of starting point of the moving bar. This means that subjects often could clear several of the repetitions even if they only found a method for moving the bar in one direction, and completion rates under 0.5 should thus be seen as having achieved little to no control of the GUI. The fact that two of the subjects started with a Completion Rate above 0.5 which then declined to under 0.5 on the second test could be either a result of muscular fatigue or simply due to chance.

5.3.1 Viability of differential activation using biofeedback training

Although the limitations of surface EMG and the experimental setup meant that it was difficult to conclusively determine whether the training yielded any improved differential activation in this experiment, the training concept and biofeedback GUI shows promise. Most subjects found the training engaging and the different tasks built in to the GUI managed to keep the subjects' attention for the duration of the training. However, if surface EMG is to be used the way the differential activation is evaluated in the GUI needs to be improved.

A straightforward way of improving the results would be to implement a weighting of the different electrodes in the computation of the COG. This would make it possible to disable electrodes covering other muscles as well as to emphasise the electrodes showing the most activity for the trained muscle. A combination of carefully chosen electrode weights and fixation of the limb should minimise effects of both muscular cross-talk, shifting of the muscular bulk and stretching of the skin.

Another issue that remains to be investigated is the timeframe for a successful voluntary differential activation training. It is possible that several training sessions during a period of days or even weeks is needed for noticeable progress to happen. As mentioned above, much of the improvement during these short training sessions can probably be ascribed to simply getting used to the GUI. A study where the improvement during several training sessions was measured could be used to analyse whether this is the case.

5.3.2 Other possible applications of the biofeedback GUI

Although the biofeedback GUI was developed with training of voluntary differential activation in mind, there are other possible applications for this type of biofeedback.

One possible such idea could be to use biofeedback in conjunction with Targeted Muscle Reinnervation (TMR) surgery. TMR is a relatively recent surgical development in

prosthetic control, introduced by Kuiken et al in 2004 [31]. TMR is the technique of reinnervating muscles or muscular compartments which are non-functional after amputation with motor nerves without function, utilising the muscles as biological amplifiers for the nerves. This allows usage of the signals from severed nerves for control of a prosthesis. Different levels of amputation utilises different muscles and motor nerves in TMR [32].

The TMR surgery is followed by a lengthy rehabilitation program to determine which movements incite optimal activation of the innervated muscles and to strengthen the target muscles [33]. This training is performed manually by palpation and the subjective sensations of the amputee. A biofeedback system could perhaps prove a valuable tool in performing this training.

Another possible idea could be rehabilitation of muscular imbalances. Certain muscular pathologies are associated with muscular imbalances, causing pain and discomfort. Biofeedback training has shown to be able to help restore these kinds of imbalances [25], making such rehabilitation a viable application as well.

5.4 Future work

An interesting area of further research would be to perform activation pattern measurements on amputee subjects. There have been previous experiments where distal movements were successfully decoded using pattern recognition on EMG collected from upper arm muscles of amputee subjects [34]. It was suggested that activity from muscle groups not originally related to the distal movement in fact stemmed from neuromuscular and/or cortical reorganization. Such phenomena would probably yield very different conditions which could be interesting to analyse in a similar study.

A limiting factor throughout the development of the biofeedback GUI was the limited performance of Matlab, limiting the number of updates per second and smoothness of the GUI. Rewriting and optimizing the GUI in a more performant language could allow a smoother and more responsive training, possibly improving the results by responding more rapidly to changes in levels of differential activation.

However, maybe more important is to develop strategies to ensure that the GUI only can be controlled through differential activation, whether through sophisticated algorithms or use of intramuscular electrodes. This is needed to ensure that the GUI trains differential activation rather than compensatory strategies sufficient for controlling the GUI.

After sufficient improvement of the GUI, a good next step with regards to the biofeedback training would be to perform a training program with several training sessions during a period of days or weeks. Apart from showing improvement over time, the additional data would give a good foundation for analysing what improvements come from increased proficiency of the GUI and what improvements actually come from increased differential activation that could be useful in the context of prosthetic control.

6 Conclusion

The project resulted in, apart from a study performed to investigate activation patterns and voluntary differential activation of the biceps brachii, improved measurement hardware and the development of two GUIs, suitable for analysing HD-sEMG data and performing biofeedback training.

The results showed clustering in the task-specific COG for all subjects, indicating consistent patterns in activation patterns within the muscle during movements. These patterns appeared to be individual for each subject. In the differential activation training, most subjects were shown to have achieved improved control of the biofeedback GUI during the training session, possibly indicating that intentional and voluntary differential activation is possible to train.

However, limitations in the surface EMG technology makes it difficult to establish for certain that the measured differential activation stems from separate activation of the compartments of the muscle. More sophisticated data processing algorithms or use of intramuscular EMG would be necessary to control for effects such as muscular cross-talk and displacement of the muscular bulk under the skin.

After improving the measurement methods, a good next step for increased understanding of the mechanics behind differential activation would be to perform activation pattern measurements on amputee subjects as well as perform a biofeedback training program during longer periods of time. This would yield increased understanding as to how the muscular activation patterns change after an amputation as well as allow investigation of how differential activation improves with training over time.

7 References

[1] C. I. Kaufman, “Limb transplantation: From a concept to reality over the last 50 years,” *J. Rehabil. Res. Dev.*, vol. 50, no. 7, p. xxvii, 2013.

[2] R. L. Segal, “Neuromuscular compartments in the human biceps brachii muscle.,” *Neurosci. Lett.*, vol. 140, no. 1, pp. 98–102, Jun. 1992.

[3] J. G. Webster and J. W. (John W. Clark, *Medical instrumentation : application and design*. John Wiley & Sons, 2010.

[4] E. D. SHERMAN, “a Russian Bioelectric-Controlled Prosthesis: Report of a Research Team From the Rehabilitation Institute of Montreal.,” *Can. Med. Assoc. J.*, vol. 91, no. 24, pp. 1268–70, Dec. 1964.

[5] P. Parker, K. Englehart, and B. Hudgins, “Myoelectric signal processing for control of powered limb prostheses,” *J. Electromyogr. Kinesiol.*, vol. 16, no. 6, pp. 541–548, 2006.

[6] A. D. Roche, H. Rehbaum, D. Farina, and O. C. Aszmann, “Prosthetic Myoelectric Control Strategies: A Clinical Perspective,” *Curr. Surg. Reports*, vol. 2, no. 3, p. 44, Mar. 2014.

[7] M. Atzori and H. Müller, “Control Capabilities of Myoelectric Robotic Prostheses by Hand Amputees: A Scientific Research and Market Overview.,” *Front. Syst. Neurosci.*, vol. 9, p. 162, 2015.

[8] A. Holtermann, K. Roeleveld, and J. S. Karlsson, “Inhomogeneities in muscle activation reveal motor unit recruitment,” *J. Electromyogr. Kinesiol.*, vol. 15, no. 2, pp. 131–137, 2005.

[9] A. Holtermann *et al.*, “Selective activation of neuromuscular compartments within the human trapezius muscle,” *J. Electromyogr. Kinesiol.*, vol. 19, no. 5, pp. 896–902, 2009.

[10] A. Holtermann, C. Grönlund, J. S. Karlsson, and K. Roeleveld, “Differential activation of regions within the biceps brachii muscle during fatigue,” *Acta Physiol.*, vol. 192, no. 4, pp. 559–567, Apr. 2008.

[11] M. Rojas-Martínez, M. A. Mañanas, and J. F. Alonso, “High-density surface EMG maps from upper-arm and forearm muscles,” *J. Neuroeng. Rehabil.*, vol. 9, 2011.

[12] M. Jordanic, M. Rojas-Martínez, M. A. Mañanas, and J. F. Alonso, “Spatial distribution of HD-EMG improves identification of task and force in patients with incomplete spinal cord injury.,” *J. Neuroeng. Rehabil.*, vol. 13, no. 1, p. 41, Apr. 2016.

[13] T. M. M. Vieira, R. Merletti, and L. Mesin, “Automatic segmentation of surface EMG images: Improving the estimation of neuromuscular activity,” *J. Biomech.*, vol. 43, no. 11, pp. 2149–2158, 2010.

[14] B. M. ter Haar Romeny, J. J. Denier van der Gon, and C. C. A. M. Gielen, “Relation between location of a motor unit in the human biceps brachii and its critical firing levels for different tasks,” *Exp. Neurol.*, vol. 85, no. 3, pp. 631–650, Sep. 1984.

[15] J. M. Brown, C. Solomon, and M. Paton, “Further evidence of functional differentiation within biceps brachii,” *Electromyogr. Clin. Neurophysiol.*, vol. 33, no. 5, pp. 301–309, 1993.

[16] C. Pérot, L. André, L. Dupont, and C. Vanhoutte, “Relative contributions of the long and short heads of the biceps brachii during single or dual isometric tasks,” *J. Electromyogr. Kinesiol.*, vol. 6, no. 1, pp. 3–11, 1996.

[17] H. Piitulainen, A. Botter, R. Merletti, and J. Avela, “Multi-channel electromyography during maximal isometric and dynamic contractions,” *J. Electromyogr. Kinesiol.*, vol. 23, no. 2, pp. 302–310, Apr. 2013.

[18] K. Watanabe, M. Kouzaki, and T. Moritani, “Spatial EMG potential distribution of biceps brachii muscle during resistance training and detraining,” *Eur. J. Appl. Physiol.*, vol. 115, no. 12, pp. 2661–2670, Dec. 2015.

[19] B. Harwood, D. L. Edwards, and J. M. Jakobi, “Age independent and position-dependent alterations in motor unit activity of the biceps brachii,” *Eur. J. Appl. Physiol.*, vol. 110, no. 1, pp. 27–38, Sep. 2010.

[20] S. K. Hunter, R. Lepers, C. J. MacGillis, and R. M. Enoka, “Activation among the elbow flexor muscles differs when maintaining arm position during a fatiguing contraction,” *J. Appl. Physiol.*, vol. 94, no. 6, pp. 2439–2447, Jun. 2003.

[21] G. W. Kroon and M. Naeije, “Recovery following exhaustive dynamic exercise in the human biceps muscle,” *Eur. J. Appl. Physiol. Occup. Physiol.*, vol. 58, no. 3, pp. 228–232, 1988.

[22] N. Nejat, P. A. Mathieu, and M. Bertrand, “Study on the activation of the biceps brachii compartments in normal subjects,” pp. 793–797, 2012.

[23] P. Aghajamaliaval, “Investigation of Dipole Sources in the Biceps Brachii as Upper Limb Position is Modified,” 2015.

[24] C. Yucha and C. Gilbert, “Evidence-Based Practice in Biofeedback and Neurofeedback,” 2004.

[25] C. D. Davlin, W. R. Holcomb, and M. A. Guadagnoli, “The Effect of Hip Position and Electromyographic Biofeedback Training on the Vastus Medialis Oblique: Vastus Lateralis Ratio,” *J. Athl. Train.*, vol. 34, no. 4, pp. 342–349, 1999.

[26] E. J. Scheme and K. B. Englehart, “Validation of a selective ensemble-based classification scheme for myoelectric control using a three-dimensional fitts’ law test,” *IEEE Trans. Neural Syst. Rehabil. Eng.*, vol. 21, no. 4, pp. 616–623, 2013.

[27] M. Ortiz-Catalan, R. Brånemark, and B. Håkansson, “BioPatRec: A modular research platform for the control of artificial limbs based on pattern recognition algorithms,” *Source Code Biol. Med.*, vol. 8, no. 1, p. 11, 2013.

[28] M. Ortiz-Catalan, B. Håkansson, and R. Brånemark, “GitHub - biopatrec/biopatrec.” [Online]. Available: https://github.com/biopatrec/biopatrec. [Accessed: 18-Sep-2017].

[29] B. Freriks and H. J. Hermens, “SENIAM9: European Recommendations for Surface ElectroMyoGraphy, Results of the SENIAM Project,” Enschede, the Netherlands, 1999.

[30] N. Nilsson, “Electromyography Analysis by Classification Complexity Estimations A Study of the Complexity of Myoelectric Pattern Recognition,” pp. 1–24.

[31] T. a Kuiken, G. a Dumanian, R. D. Lipshutz, L. a Miller, and K. a Stubblefield, “The use of targeted muscle reinnervation for improved myoelectric prosthesis control in a bilateral shoulder disarticulation amputee,” *Prosthet. Orthot. Int.*, vol. 28, pp. 245–

253, 2004.

[32] B. T. Carlsen, P. Prigge, and J. Peterson, “Upper extremity limb loss: Functional restoration from prosthesis and targeted reinnervation to transplantation,” *J. Hand Ther.*, vol. 27, no. 2, pp. 106–114, Apr. 2014.

[33] K. A. Stubblefield, L. A. Miller, R. D. Lipschutz, and T. A. Kuiken, “Occupational therapy protocol for amputees with targeted muscle reinnervation,” *Journal of Rehabilitation Research and Development*, vol. 46, no. 4. JOURNAL REHAB RES & DEV, BALTIMORE, pp. 481–488, 2009.

[34] N. Jarrasse *et al.*, “Classification of Phantom Finger, Hand, Wrist and Elbow Voluntary Gestures in Transhumeral Amputees with sEMG,” *IEEE Trans. Neural Syst. Rehabil. Eng.*, pp. 1–1, 2016.